NTNU
Norwegian University of
Science and Technology

Liquinert quartz crucible

Removal of OH groups in silica crucibles to reduce wetting between the crucible and the silicon melt

Mathias Strømmen

Chemical Engineering and Biotechnology
Submission date: June 2018
Supervisor: Marisa Di Sabatino, IMA
Co-supervisor: John Atle Bones, SINTEF

Norwegian University of Science and Technology
Department of Materials Science and Engineering

Acknowledgements

I would like to thank my supervisor Marisa Di Sabatino Lundberg and co-supervisors John Atle Bones (SINTEF) and Astrid Marie Muggerud (The Quartz Corp) for their help, discussions and feedback throughout the project. I would also thank Nicholas Smith for helping me with the TGA Furnace. I especially want to thank Sarina Bao (SINTEF) and Bendik Sægrov-Sorte (SINTEF) for their help and patience when it comes to the wetting furnace. They have provided a lot of good discussions and tips. And last, but not least, I would like to thank Birgitte Karlsen. You didn't actually help me much, but you saved me a lot of time.

Trondheim, July 2018
Mathias Strømmen

Table of Contents

Abstract

When producing monocrystalline silicon ingots for the solar cell industry quartz crucibles are most commonly used. A quartz crucible used in the Czochralski (CZ) process will be used to pull ingots for more than 100 hours. During this time, some of the crucible will dissolve into the melt, along with any impurities in the crucible. To avoid this, the a liquid inert (liquinert) crucible can be used. This master thesis investigate two different crucible types, one fused quartz crucible made from natural quartz, and one crucible made from synthetic quartz. The focus have been on removing hydroxyl (OH) groups from the crucible by heat treatment, and to see how this effects wetting between the crucible and silicon. Some samples were also coated, to investigate the effect of coating and wettability. Samples have been taken from the inner surface of the crucibles, and polished. Heat treatment have been done in three different furnaces, a Sliding Flanges Tube (SFT) furnace, Alumina Tube Furnace (ATF) and in a Thermal Gravimetric Analysis (TGA) furnace, under vacuum conditions. As expected, heat treatment under vacuum conditions reduced the OH content in the samples. When heat treated at temperatures at and above 1450 ℃, a significant amount of cristobalite is formed. The non-coated samples showed a clear negative correlation between the OH content and wetting angle. For the coated samples there were too many uncertainties to identify a correlation between the wetting angle and the OH content. However, the coated samples had a generally higher wetting angle than the non-coated samples. The work done in this thesis did not produce a liquinert crucible, but by reducing the OH content in the crucible, the wetting angle was increased, which may be a step in the direction of creating a liquinert quartz crucible.

1 Introduction

1.1 Motivation

When it comes to the global solar cell marked, silicon is essential, as it is the most used material for commercial solar cells and ingots. Cells from multicrystalline and monocrystalline silicon ingots combined contributes to about 90% of the marked [1]. Fused silica crucibles are also the most commonly used crucible when producing monocrystalline silicon ingots, while slip cast crucibles are used when producing multicrystalline ingots. This work will focus around fused silica crucibles. When it comes to quality, monocrystalline ingots are superior to multicrystalline ingots. The amount of defects are lower, the purity is higher, and the peak efficiency is higher. Monocrystalline ingots are usually made with the Czochralski growth method, where a seed crystal is added to the silicon melt to initiate crystallization, and then the ingot is slowly pulled up from the melt, creating one large single crystal. During this process a significant amount of the silica crucible is dissolved, due to the high temperature of the melt. Due to this, the crucible is only used twice before it is considered unusable and thrown away. High quality silica crucibles are not cheap, and since they are only used twice, the price of the crucible will reach upwards to 30% of the total wafer cost [2]. Finding a way to increase the times the crucible can be used, would significantly reduce the production costs, and reduce the amount of impurities that come from the dissolved crucible.

Crystalline quartz can be found in nature with high purity, has a high thermal resistance, low thermal expansion and high resistance to thermal shock, as well as high softening temperature, and when melted makes silica, which is very suitable to be used as crucible material. When silica is heated to high temperatures, the crystal structure changes, and cristobalite is formed. The cristobalite layer works as a protective layer for the quartz crucible, as it has a higher viscosity than quartz, much like the aluminum oxide layer on aluminum. This causes the crucible to be less effected by the increased softening that happens to the silica at higher temperatures. The phase transformation from silica to cristobalite is unavoidable at these temperatures. Some of the crucible will dissolve into the melt, and thus the impurities from the crucible will end up in the melt. It is important that the cristobalite layer is even and smooth. If it breaks, the silicon can get through and behind the cristobalite layer, and cause the layer to flake off, which can lead to defects and structure losses at the solidification front of the monocrystal. In order to get a smooth cristobalite layer, the inner surface of the crucible is coated or doped with a devitrification agent. The devitrification agent reacts with the quartz at high temperatures and form nucleation sites that promotes the phase transition from quartz to cristobalite.

The crucible consists of two layers, the outer and the inner layer. The outer layer is more porous, with bubbles, and the inner layer is bubble free and smooth. The amount of crucible that is dissolved into the melt has a direct effect on the purity of the produced silicon, as the crucible contains oxygen, that reacts with the graphite in the heaters, which again increases the amount of carbon impurities in the melt. A perfect liquid inert, so called liquinert, crucible, will not dissolve into the melt at all, and last indefinitely. A perfect liquinert crucible does not exist, but it is possible to make the crucible less reactive to the melt. By reducing the wettability of the crucible, the amount of the crucible

that dissolves into the melt will be reduced, by making it more liquinert. To reduce the wettability of the crucible, the level of OH-groups is reduced by heat treatment by out diffusion. A more liquinert crucible will increase the purity of the melt, and may increase the lifetime of the crucible, which will lead to better and cheaper solar cells. This is the motivation of the project, to come closer to making a crucible that will withstand the Czochralski method better, thus making more efficient and cheaper solar cell.

1.2 The aim of this work

The aim of this work is to come one step closer to making a liquinert crucible. This will be done by removing OH groups from the silica by heat treatment, and investigate how the wettability between the silicon melt and the crucible is effected by this. The samples were heat treated at different temperatures, different holding times, and different atmospheres, to see how the OH content changed. To measure the OH content FTIR spectroscopy was used. Some samples were also coated with $Ba(OH)_2$ after heat treatment to investigate wettability effects caused by coating and different OH contents. The wettability of the samples were measured in a wettability furnace, and compared.

1.3 List of abbreviations

- **BC**: Bubble Containing
- **BF**: Bubble Free
- **CZ**: Czochralski
- **EBSD**: Electronic backscatter diffraction
- **FTIR**: Fourier Transform Infrared Spectroscopy
- **ICP-MS**: Inductively coupled plasma mass spectrometry
- **Liquinert**: Liquid inert
- **MCZ**: Magnetic-field applied Czochralski
- **Natural**: Crucible made from natural quartz sand
- **ppm**: parts per million
- **SEM**: Scanning Electron Microscope
- **SFT**: Sliding Flanges Tube
- **Synthetic**: Crucible made from synthetic quartz sand

2 Theory

2.1 Quartz

Silica and quartz are often used interchangeably, but for this work quartz will be defined as the crystalline mineral, and silica as amorphous glass. Crystalline quartz is a very common material, and can be found in many different geological environments. [3]. Pure crystalline quartz is colorless and transparent, and its melting point is at around 1705 ℃, while pure silicon has a melting temperature of 1414 ℃. Our Earth is literally covered with quartz, and a total of 12% of the Earth's crust is quartz. Pure quartz is needed to produce glass, optical fibers, chemical apparatus and ceramics, as well as a key ingredient in concrete and in computer microchips.

There are 11 crystalline polymorphs of silica that can occur, some of them shown in the phase diagram of silica in Figure 1. All the different phases have the same chemical composition, SiO_2, but different phases occurs under different pressures and temperatures. The properties of the different phases also vary, i.e. thermal expansion [4].

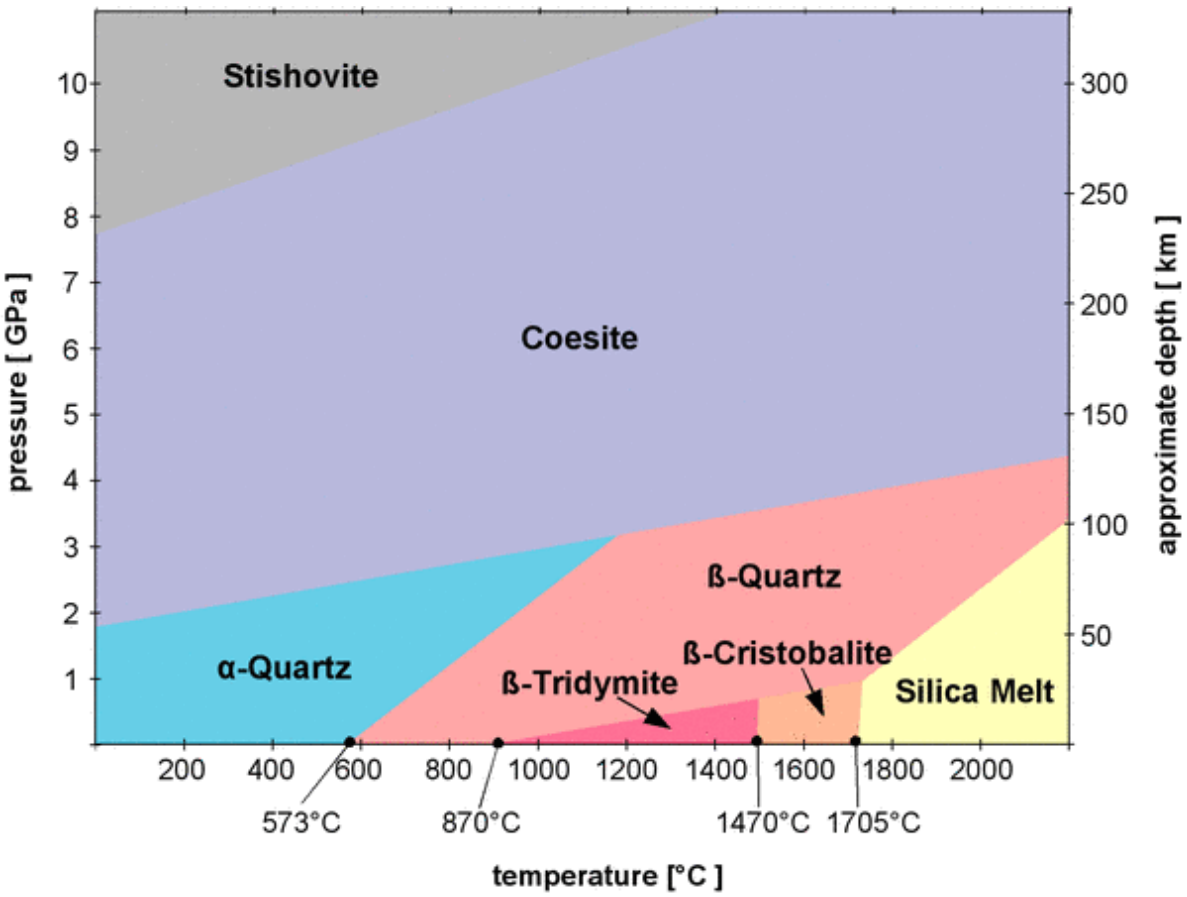

Figure 1: Phase diagram of silica.[5]

When the melt is cooled quickly, no phase transformation will happen, and it will stay as an amorphous silica glass. When silica glass is heated, it will not go through phase

transformations to β-Quartz or β-Tridymite, as expected from the phase diagram,, but only β-Cristobalite, which will start to form slowly at about 1000 ℃, before melting at about 1705 ℃.

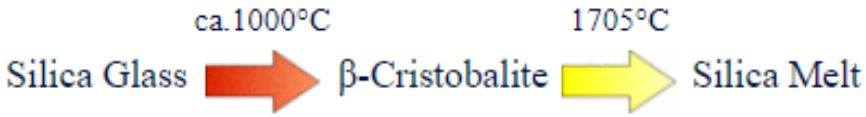

Figure 2: Phase transformation of silica glass to silica melt through β-Cristobalite.[5]

When producing silica glass, there is always a possibility that β-Cristobalite is created within the glass, which will start to form at approximately 1000 ℃. To create fused silica, pure SiO_2-glass, a continuous process of flame oxidation is present, to make volatile silicon compound into SiO_2 dust, and then fuse the dust into the glass. This can be done with both a gas-fuelled furnace, and an electrically heated furnace, resulting in flame-fused and electrically fused silica glass respectively.

When creating fused silica glass, small bubbles can be trapped inside the glass. The size of the bubbles are dependent on the OH-content and the rate of the cooling. The entire process effects the properties of the silica glass.

2.2 The Czochralski process

The Czochralski process is a method to grow single crystals of materials, a monocrystalline solid. It can be semi-conductors, metals, gemstones or salts, only requiring the material to be crystalline. In a monocrystalline solid the crystal structure is close to perfect, and the arrangement of the atoms are at a given order across the entire crystal. The Czochralski process was invented in 1915 by the Polish scientist Jan Czochralski and is still being used in industrial production of monocrystalline silicon. Monocrystalline silicon, (single crystal) sc-Si, is in almost every single electronic device that exists, and in 2016, 20.2 % of all solar cells produced from sc-Si [1]. Solar cells produced from sc-Si generally has better efficiency than polycrystalline silicon, (multicrystalline) mc-Si.

The following chapter describes the general principle of operation of the Czochralski process [6]. The desired material is placed in a crucible, and the crucible is then loaded into a furnace, and heated to well above the melting temperature of the material. To ensure even heat distribution, the crucible is continuously rotating. As the heating elements often are made of graphite, the entire furnace contains an inert gas, to avoid the heating elements burning, and at low pressures. When producing sc-Si, the pressure in the Czochralski puller is close to 30 mbar. After everything has melted, and the melt is even, the temperature is decreased to just above the melting point. A seed crystal is then inserted, and when the seed touches the melt, the melt solidifies immediately around the seed, and takes on the same crystal orientation as the seed [7]. The seed is then slowly

pulled up from the melt, and the melt that is directly below, and touches, the solidified material, is also solidified, due to surface tension. The diameter of the ingot is dependent on the rate the seed crystal is pulled. The ingot is then slowly pulled all the way, until there is almost no melt left in the crucible. A schematic drawing of the Czochralski process for producing sc-Si is showed in Figure 3.

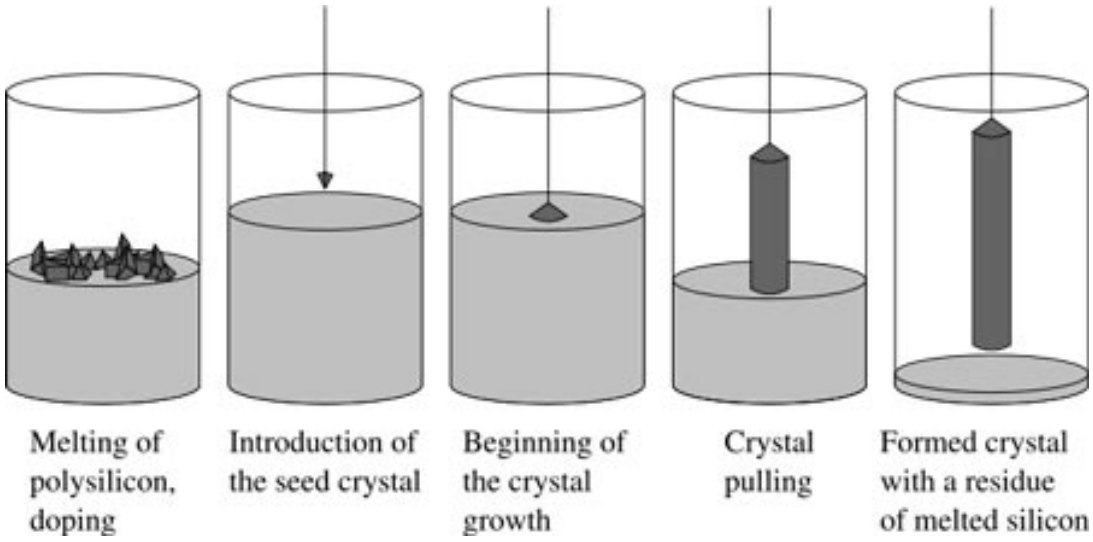

Figure 3: Schematic picture of the Czochralski process used to make sc-Si [8].

When the melt is precipitating at the seed crystal, only the silicon solidifies, since this is the atoms that will "fit" in the crystal lattice of the seed. This means that the impurities will stay in the melt, and as the ingot is pulled out, the concentration of impurities are increased in the melt. The temperature in the melt is high, and due to this, some of the crucible will be dissolved into the melt as well, together with the impurities.

2.3 The effects of coating on crucibles

As the formation of cristobalite is unavoidable, a way of controlling the formation is necessary. A possible way to do this is by coat or dope the surface of the crucible with a devitrification agent. Doping will not be addressed in this thesis. At high temperatures the devitrification agent will react with the silica glass, and creates nucleation where the phase transition from silica to cristobalite will occur at a greater rate. This will make the cristobalite layer grow radially and form an even and uniformly [9, 10].

Alkaline-earth elements are suited as a devitrification agent, due to the fact that they can form oxides, carbonates and silicates. Another important requirement for the devitrification agent is that it should not be a source of impurities into the melt. For the solar industry, barium is commonly used. There are two main types of coating used, dip coating and spray coating. Industrially, spray coating is more commonly used than dip coating. In this thesis, only spray coating will be covered. It has been shown that when a silica crucible wall is coated with saturated barium hydroxide ($Ba(OH)_2$) the

coating reacts with the carbon dioxide in the air and create barium carbonate ($BaCO_3$) [11]. When the barium carbonate is heated it will decompose into barium oxide, and the barium oxide will react with the silica glass and form barium silicate ($BaSiO_3$). This is the nucleation site were the cristobalite is formed. Due to the high toxicity of barium, the coating process must be handled with care.

Industrially the coating will be done by large spray coating machines that spreads the coating evenly on the entire surface, including the outside, of the crucible. This is done to increase the shell effect the more viscous cristobalite gives the crucible. An ultrasound nozzle breaks the solution into micro droplets, and is sprayed onto the surface. The final coating has been investigated and a SEM image of an industrially coated crucible can be seen in Figure 4[12].

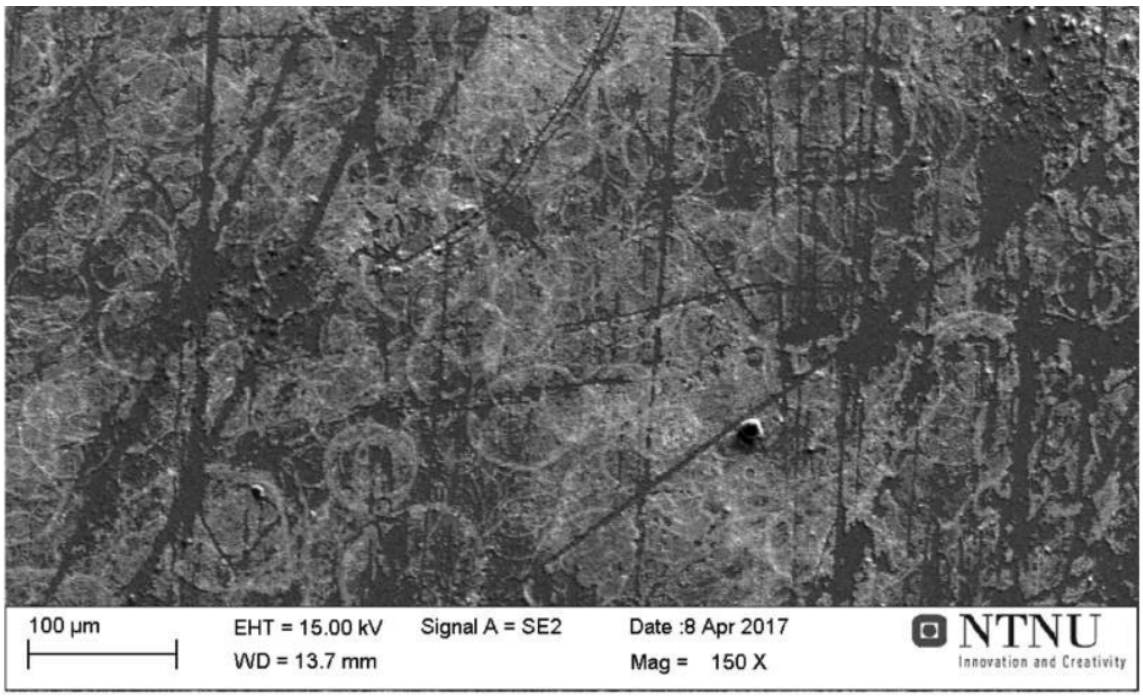

Figure 4: SEM image of a crucible piece industrially coated with $Ba(OH)_2$ at a magnification of $150X$ [12].

The white rings observed in Figure 4 are a result of the coating. The chemical composition of the white rings were obtained, and confirmed that it contains barium. The coating is easily removed, and and must be handled with care.

2.4 Crucibles for CZ monocrystalline silicon production

The crucible used in the Czochralski process are made from fused silica. The exact process of creating the fused silica crucibles are kept a secret by each producer, but the general method can be found in patents [13].

High purity quartz sand is added to a mold, which is rotating around its vertical axis. The mold is usually made of graphite, due to its low cost, availability, and its ability

to withstand high temperature, as well as being a good thermal and electric conductor. Because of the centrifugal forces that appear when the mold is rotating and a shaping tool, similar to a large rubber spatula, the sand will be evenly spread around the mold with even thickness. There are small holes on the entire mold, where vacuum is applied. The vacuum sucks out most of the gasses that are in the sand when it is being melted.

The procedure follows the following steps. Quartz sand with similar sized grain size is spread evenly in the rotating mold, with the wanted thickness. The low vacuum is turned on, and the heater is inserted into the mold. The heater gradually melts the sand, and the vacuum removes any gas released by the melting grains. This creates the Bubble Free (BF) layer of the crucible. When the BF layer has the desired thickness, the vacuum is turned of. The melting front will still move towards the outside of the crucible, but any gas stuck in between the sand grains will be stuck. This creates the Bubble Containing (BC) layer. Right before all the sand has melted, the heater is turned of, and some quartz sand is left. This is to make the removal of the crucible from the mold easier. In Figure 5 the production set up is shown.

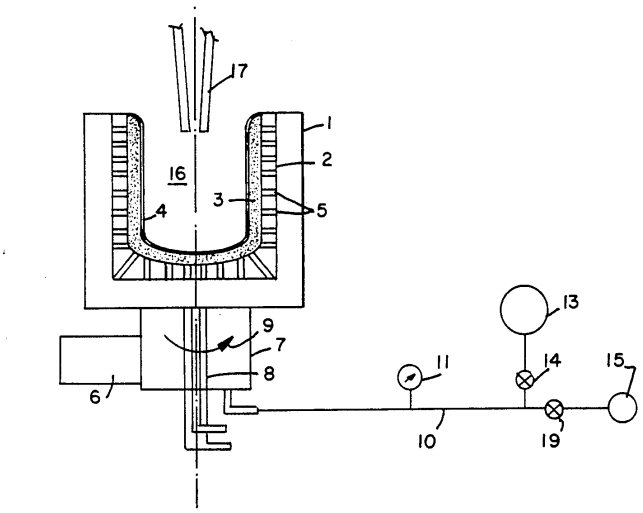

Figure 5: Production of quartz crucible. The heater(17), the BF layer (4), and the BC layer (3) [13].

As mentioned in the previous chapter, some of the crucible will dissolve into to melt. For an industrial crucible that has been used to pull two ingots, approximately 1-2 mm of the crucible will have dissolved into the melt. In weight, this equals about 2 kg [12]. As the crucible has a about 30 ppm impurities, this accounts for a non-negligible part of the impurities in the melt, especially at the end of the cycle.

2.4.1 Liquinert crucible

A recent concept crucible, a liquid inert, so called liquinert, crucible is a crucible that is less reactive with the melt. [14]. In one Czochralski process, superconductive magnets can be used to apply a magnetic field to the melt, which will make the grown silicon have a lower oxygen content than ingots made without the magnetic field. This process is

expensive. However, the Czochralski process, with a special liquinert silica crucible may be used, were the inner surface is treated to have a melt-phobic effect, and no magnetic field is applied. This is currently just in the research phase, and has not been used for industrial production of monocrystalline silicon ingots.

Two silicon ingots were made, one from the conventional Czochralski method with magnetic field (MCZ) and one with the liquinert crucible with no magnetic field applied. In Figure 6 shows the oxygen concentration in the silicon as a function of the fraction solidified. This happens due to less of the SiO_2 crucible being dissolved into the melt.

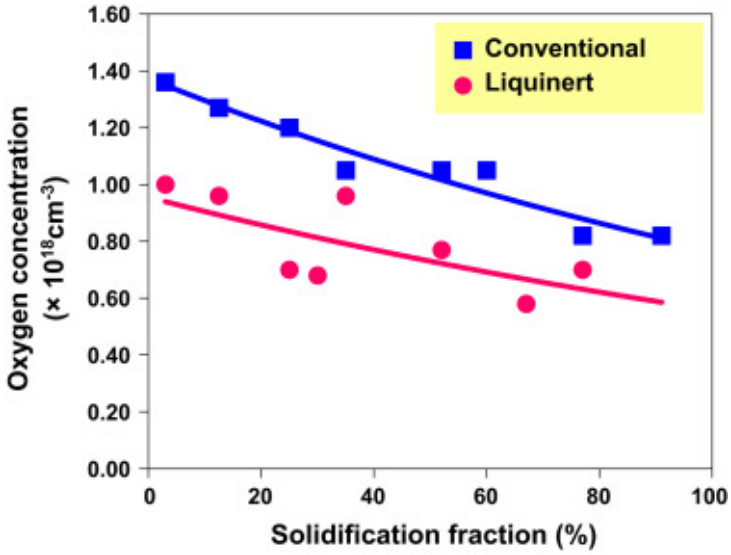

Figure 6: Oxygen concentration vs solidification fraction for two types of ingots [14].

Oxygen that is being dissolved from the SiO_2 and into the melt forms SiO, which evaporates from the melt surface. The evaporated SiO reacts with the graphite parts of the furnace, i.e the crucible support, the heater and the shield, and creates carbon monoxide (CO). The mechanism is shown in Figure 7.

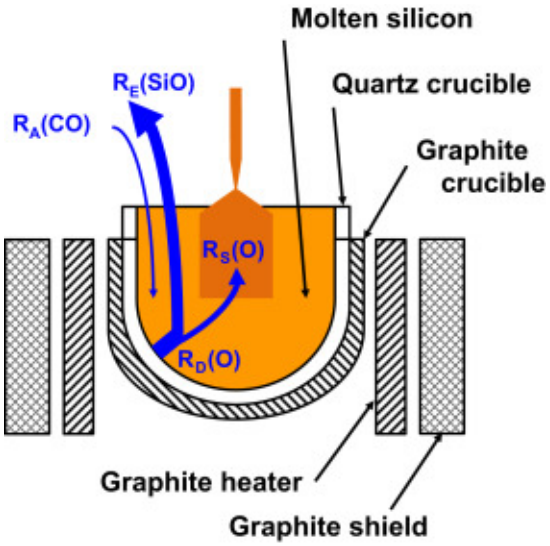

Figure 7: The reaction paths of oxygen. $R_S(O)$ is the oxygen that is incorporated into the silicon, $R_D(O)$ is the oxygen dissolved from the crucible, $R_\epsilon(SiO)$ is the evaporated SiO, and $R_A(CO)$ is the oxygen that is absorbed into the melt from CO[14].

This causes the carbon concentration in a MCZ ingot to be higher than in a ingot made with a liquinert crucible. This can be seen in Figure 8

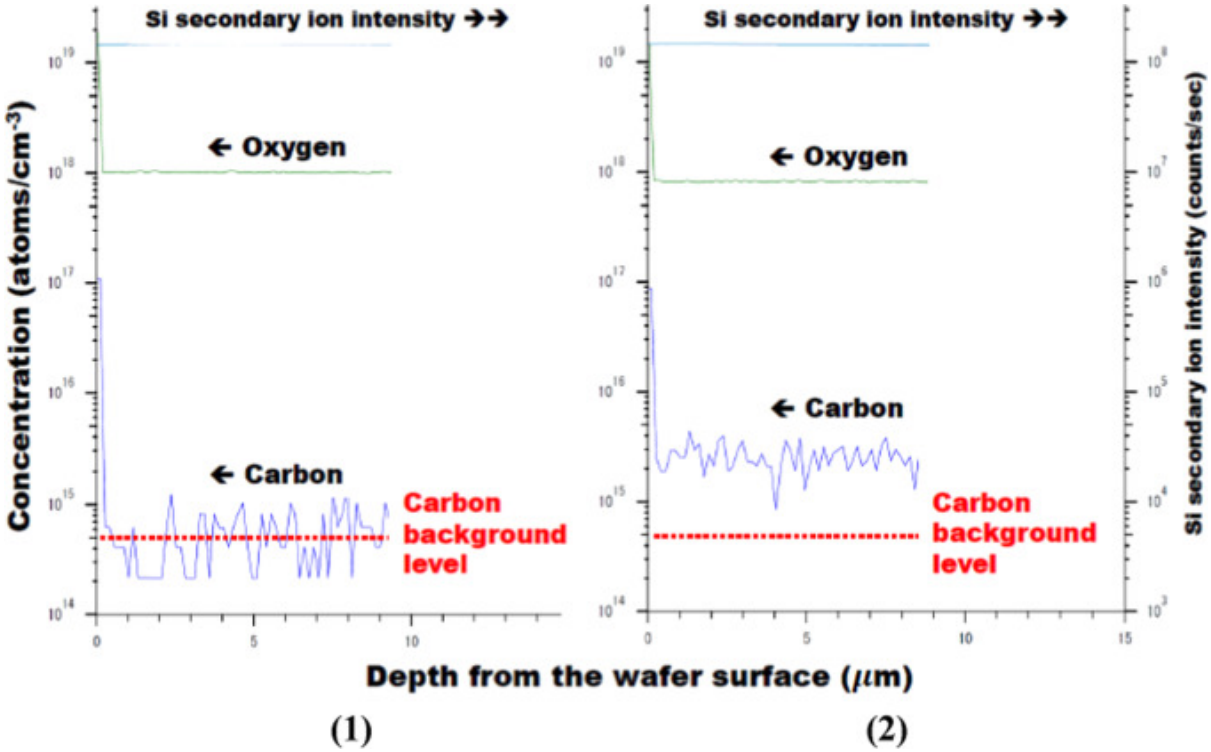

Figure 8: The concentration of carbon and oxygen in MCZ wafers and wafers from a liquinert crucible at different depths [14].

As the amount of carbon impurities increases, the lifetime of the minority carriers in

wafers is reduced. For the conventional Czochralski wafer, the lifetime is between 300 and 400 µs, while the lifetime in the wafer made in the liquinert crucible is between 700 and 800 µs. This is a one study only research, and is not yet commercial.

2.5 Diffusion in solids

In all materials, atoms move when the temperature is above 0 Kelvin. These movements are random, and cause diffusion. The rate of diffusion vary from material to material. There are two ways diffusion can occur, vacancy diffusion and interstitial diffusion. Vacancy diffusion happens when the diffusing atom is a part of the lattice, and is of similar size as the lattice atoms. It can then travel between vacancies. Interstitial diffusion occurs when a small atom is in an interstitial position in the lattice, and travels between other interstitial positions. A schematic figure is shown in Figure 9

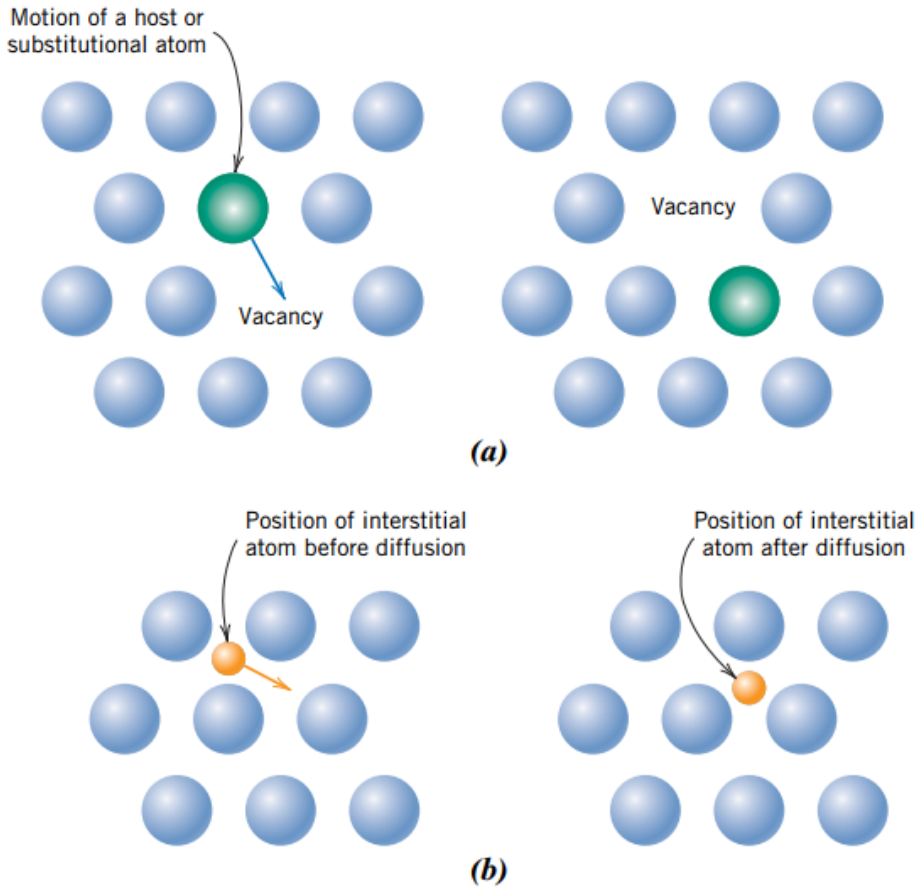

Figure 9: (a) Vacancy and (b) interstitial diffusion. [15]

The rate of non-steady diffusion of a material into a substrate can be calculated by Fick's second law, which is the two dimensional equivalent of Fick's first law.

$$\frac{\partial C}{\partial t} = D\frac{\partial^2 C}{\partial x^2} \tag{1}$$

Where C is the concentration, x is the distance within the solid, and D the diffusion

coefficient, which differ from each material.
With the assumptions of the initial concentration, C_0, is evenly distributed, and the value at the surface, x=0, is zero, equation 1 can be rewritten as

$$\frac{C_x - C_0}{C_s - C_0} = 1 - erf\left(\frac{x}{2\sqrt{Dt}}\right) \tag{2}$$

where C_x is the concentration at depth x after time t, C_0 is the initial concentration, C_S is the concentration at x=0, and erf() is the Gaussion error function, and is defined as

$$\text{erf}(z) = \frac{2}{\sqrt{\pi}}\int_0^z e^{-y^2}dy \tag{3}$$

and the values can be found in different mathematical tables.

2.5.1 Diffusion of hydroxyl groups in silica

When heat treating to remove water from silica glass, the concentration C_S is set to zero, and equation 3 can be written as

$$C_x = C_0\text{erf}\left(\frac{x}{2\sqrt{Dt}}\right) \tag{4}$$

When quartz reacts with water, the OH-groups arranged in the lattice as shown in Figure 10

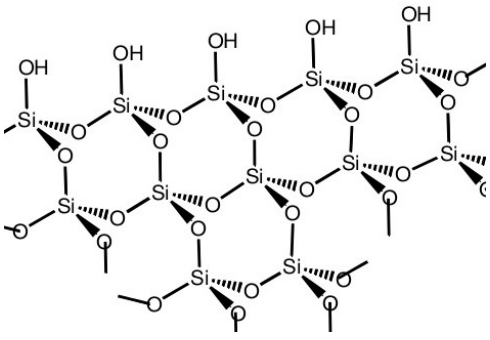

Figure 10: The OH - groups in a SiO_2 lattice.[16]

The reaction between silica and water is believed to be as seen in equation 5.[17][18]

$$\equiv\text{Si}-\text{O}-\text{Si}\equiv + \text{H}_2\text{O} \rightleftarrows \equiv\text{SiOH} + \text{OHSi}\equiv \tag{5}$$

However, when silica glass is heat treated, the amount of gasses that leave the sample is both water and hydrogen [19]. This leads to the theory that the reaction in equation 6 occurs when removing water from silica glass, based on empirical data.

$$\equiv\text{Si}-\text{OH} + \equiv\text{SiH} \longrightarrow \equiv\text{Si}-\text{O}-\text{Si}\equiv + \text{H}_2 \tag{6}$$

This happens when the temperature is above 700 ℃ [20]. When removing OH-groups from quartz tubes with a wall thickness of 1.2 mm, the tube is heated to 1060 ℃ and kept there for 40 hours under vacuum. This lowers the OH-content from 130 ppm to 0.1 ppm [21].

2.6 Wetting

When a small drop of liquid is placed on a flat solid, the shape of the drop is determined by two different forces, gravity and surface forces. The gravitational forces will try to flatten the drop, and the effect gravitational forces have on the structure is hard to calculate. However, the effect of gravity is dependent on the weight of the drop, and with small enough drops, gravitational forces can for most means be neglected. The other force is the surface force. It is determined by the relative size of the interfacial tensions between the solid and the gas phase, γ_{sg}, the solid and liquid phase, γ_{sl} and the liquid and gas phase, γ_{lg}[22].

Cohesive force (W_c) and the force of adhesion (W_a) are the inter molecular forces between similar molecules and the inter molecular forces between not similar molecules respectively. If $W_c > W_a$, it will remain in an equilibrium state, and form a drop. The shape of the drop is determined by γ_{sg},γ_{sl} and γ_{lg}. The relative size of these parameters decides and contact angle (Θ), which is defined as the angle between the tangent at the "three phase" point and the surface, as shown in Figure 11.

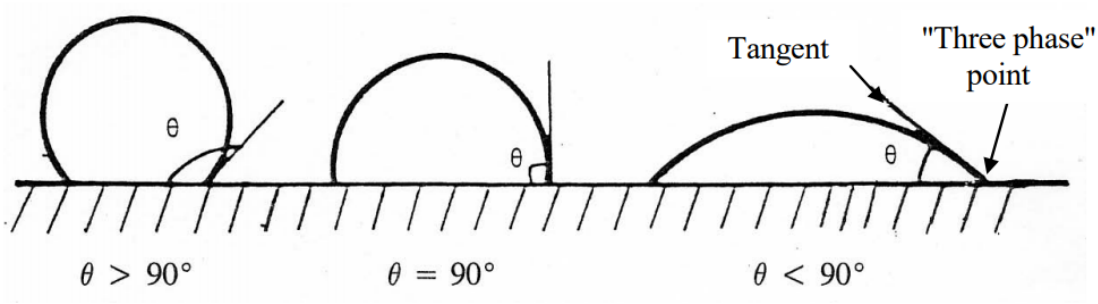

Figure 11: Cross section of different droplet shapes on a solid surface [22].

Considering an infinitesimal reduction of the droplet size, the area of the droplet will change, and the resulting reduction of surface energy can be calculated.

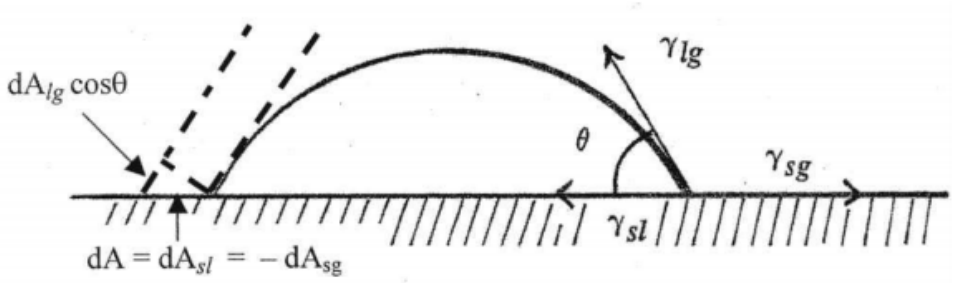

Figure 12: Cross section of a arbitrary droplet [22].

The reduction of surface energy, using the same nomenclature as in Figure 12, can be written as shown in equation 7.

$$\mathrm{dG} = \gamma_{sl} \cdot \mathrm{dA} + \gamma_{lg} \cos\Theta \cdot \mathrm{dA} - \gamma_{sg} \cdot dA \tag{7}$$

In equation 7 dG is the change in Gibbs free energy. For a system in equilibrium, the change in Gibbs free energy is zero, simplifying it to equation 8.

$$\gamma_{sg} = \gamma_{sl} + \gamma_{lg} \cdot \cos\Theta \tag{8}$$

This gives a direct relation between the contact angle, Θ, and the surface tensions, γ_{sg},γ_{sl} and γ_{lg}. Equation 8 is known as Young's equation [22]. Young's equation assumes that the surface is completely flat, but it shows that the when the contact angle is increased, the forces acting between the liquid and the surface are reduced, and consequently the reactivity between the liquid and the surface is reduced. This is the key phenomenon that will be investigated in this work. The wetting angle will not be at equilibrium when the sample has melted, but will stabilize over time [23].

2.6.1 Wetting in the silicon/silica glass interface

During the CZ process, the wetting between the silicon melt and the silica glass crucible is important to take into account when talking about oxygen transport. At the high temperatures where the CZ process takes place, some of the silica glass crucible will dissolve into the melt, and from there into the growing silicon crystal [24]. When a quartz crucible is corroded in this process, it follows the reaction in equation 9

$$\mathrm{Si\ (l)} + \mathrm{SiO_2\ (s)} \longrightarrow \mathrm{SiO\ (g)} \tag{9}$$

If oxygen leaves the melted silicon as SiO (g) under vacuum, periodic wetting and dewetting cycles can be observed [25]. When a amorphous silica glass substrate and melted silicon is investigated in a wetting furnace from the top, the drop will be a perfect circle that periodically changes size. When the same is done with a crystalline quartz substrate, a the circle becomes slightly hexagonal, due to the crystallinity of the quartz.

2.7 Characterization

2.7.1 FTIR spectroscopy

Fourier-transform infrared (FTIR) spectroscopy is a characterization technique to obtain an infrared spectrum of a material, and FTIR works on liquids, solids and gasses. The

Fourier-transform term comes from the necessity to use Fourier-transform on the raw data in order to get the infrared spectrum. The infrared region is 12800 - 10 cm^{-1} [26]. The IR - spectrum is the molecular vibrational spectrum. When a sample is exposed to infrared radiation, molecules in the sample selectively absorb radiation of a specific wavelength. This causes the dipole moment of the molecules to change, and at the same time, causes the vibrational energy levels of the molecules to excite from the ground state to the excited state, and each vibration energy is characteristic of the type of bond and molecule, giving a footprint of the compound that is present in the matrix.

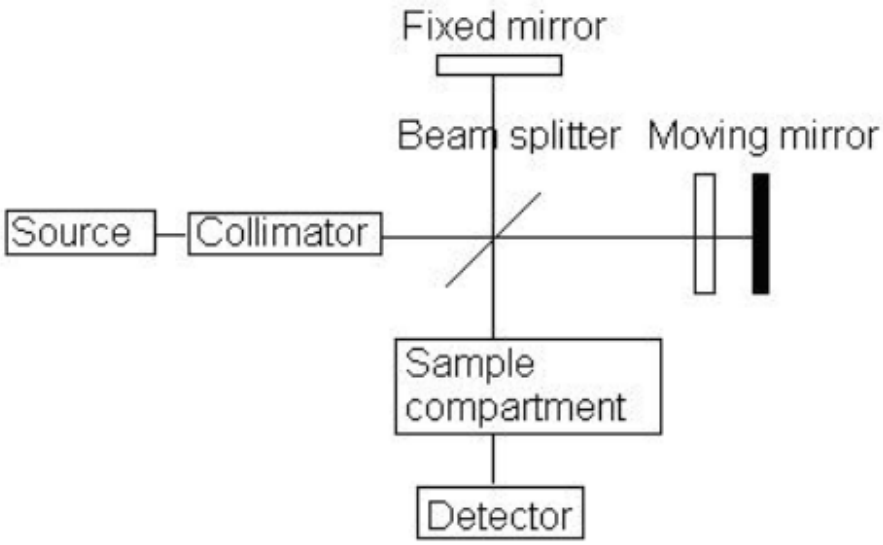

Figure 13: Schematic view of an FTIR spectrometer [26].

For any type of absorption spectroscopy, the goal is to measure how well a material absorbs light at a specific wavelength. Dispersive spectroscopy sends a monochromatic beam of light, at each wavelength, and measures how much is absorbed. For the FTIR, a polychromatic beam is sent through the sample, with many frequencies, and analyzed on a computer. The frequencies then changes, which gives new data points. This is done several times, before all the data goes through Fourier-transform, and a IR-spectrum comes out. A standard FTIR spectrometer consists of a source, sample compartment, detector, interferometer, amplifier, A/D converter and a computer. The difference between a dispersive spectrometer and a FTIR spectrometer is the interferometer. In FTIR spectroscopy a Michelson interferometer is used, which splits the light in two, so the paths are different, and recombines them. This is done with a beam splitter and a moving mirror. A schematic view of an FTIR spectrometer can be seen in Figure 13.

2.7.2 Scanning electron microscope

Normal microscopes are insufficient when it comes to seeing in the micron-nanometer range. To be able to collect information in this range, a scanning electron microscope (SEM) has to be used. A SEM uses electrons instead of photons. Electrons can have shorter wavelength than photons, and can thus enable better magnifications then classical light microscopes. A SEM has the following components [27]

- An electron source
- Condenser lenses
- Scanning coil
- Specimen chamber
- Detectors
- Operation Unit

The general setup for a SEM can be seen in Figure 14. The electrons are produced at the top of the column, by thermionic heating. Commonly is a Tungsten filament used [28]. The electrons are then accelerated through the lenses, which focuses the electrons to a narrow beam. As opposed to glass lenses used in light microscopes, the SEM uses magnetic lenses to focus the electron beam. When the beam has been focused, the scanning coil redistributed in the X and Y axis in order to scan the sample in the chamber. For most SEMs the specimen chamber is evacuated to vacuum. The sample is mounted onto the stage, and can freely be moved during operation.

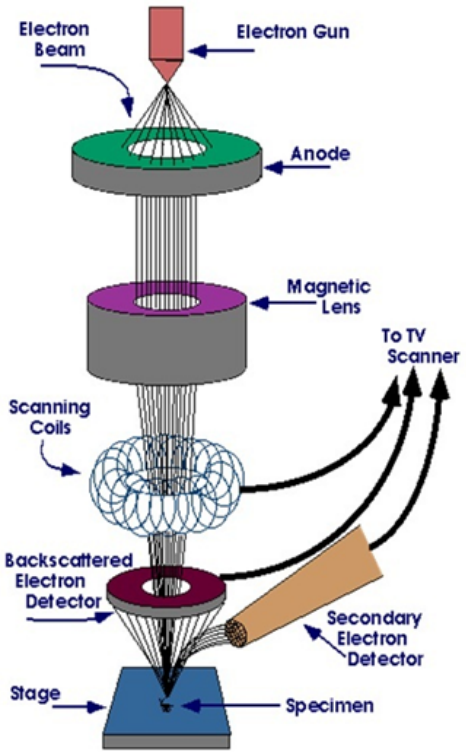

Figure 14: A general setup for a SEM [29].

The electron penetrates the sample to approximately 1 micron, thus makes the topography, morphology and composition of the surface material easily obtained. For the imaging, two types of detectors are typically used: The Secondary Electron Detector and the Backscattered Electron Detector.

Secondary electrons are electrons with low energy that are produced when electrons are ejected from the k-orbitals in the sample by the scanning beam. A detector with a Faraday cage then accelerates these electrons towards the scintillator. This makes a current which a photomultiplier detects and the amplified signal can be read on the operation unit.

Backscattered electrons are electrons with higher energy. These electrons are elastically backscattered by the sample atoms. Higher atomic number atoms has a higher backscatter efficiency. This can be used to gather compositional information about the sample. The Backscattered Electron Detector is either a scintillator or a semiconductor.

2.8 Measuring OH content in silica glass

To measure the OH content in silica glass, FTIR - spectroscopy is used. The method described in this chapter is made based on the results from a Bruker Vertex 80v FT-IR. The Silanol hydroxyl groups in the silica glass is characterized with from the absorption band at λ = 2.7 - 2.85 μm, or equivalently wavenumber ν = 3500-3700 cm^{-1} [30]. To calculate the OH content, three steps are necessary [31].

The first step is to find find the baseline. This is needed to calculate the peak height of the OH absorption at the given wavenumber. The baseline is found most accurately using a Spline (Bézier) polynomial. The second step is to find the largest different between the baseline and the spectrum, T_{min}, the minimum transmission. The third and final step is the OH - calculation, and is based on Lambert-Beer's law, which can be written

$$\beta = \frac{1}{d} \cdot log_{10}\left(\frac{T_{max}}{T_{min}}\right) \tag{10}$$

Where β is the optical density, d is the width of the sample, and $T_{\text{max/min}}$ is the max/min transmission. The T_{max} can be found by adding the peak height to T_{min}, and the OH content can then be measured

$$\text{OH(ppm)} = \beta \cdot \text{factor} \tag{11}$$

where

$$\text{factor} = \frac{M_{\text{OH}} \cdot 10,000}{\epsilon\text{OH} \cdot \rho_{glass}} \tag{12}$$

where M_{OH} is the molar mass of OH (g/mole), ϵOH is the absorption coefficient (L mole^{-1} cm^{-1}), and ρ_{glass} is the density of the glass (g cm^{-3}).

3 Experimental

3.1 Sample material

The primary material investigated in this work was quartz crucible made from natural quartz sand and a crucible made from synthetic quartz. The crucible pieces are made of two layers, one with low bubble content, that is transparent, and a bubble containing layer, which is not transparent. The inner surface of the crucible is smooth. The glass has an absorption coefficient $\epsilon = 77.5\text{L mole}^{-1}\ \text{cm}^{-1}$ and a density $\rho = 2.20\ \text{g cm}^{-3}$. A cross section of the natural-crucible is shown in Figure 15. The synthetic crucible has the same layers, but a higher bubble count the the BF layer, as can be seen in chapter 3.2.1.

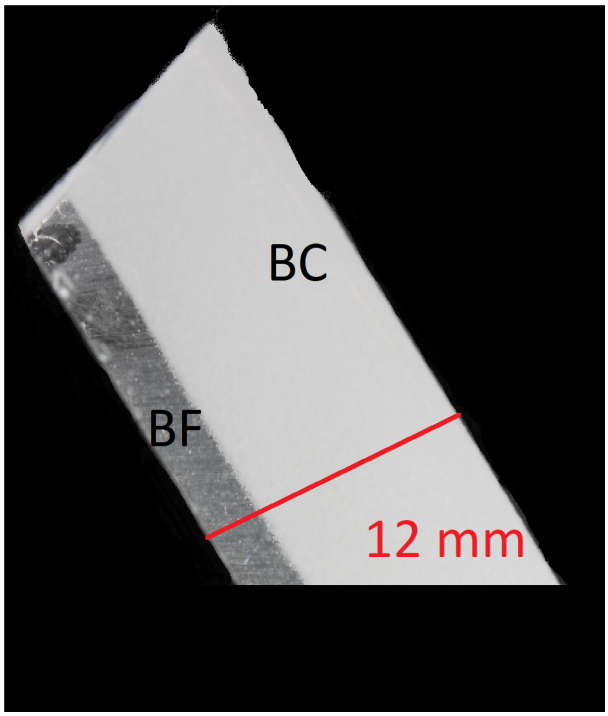

Figure 15: Cross section of the crucible, showing the BF layer and the BC layer.

The two different crucible types had different composition, and were made from different quartz, one from natural quartz and the other from synthetic, and had different production methods. The differences in alkali concentration and initial OH concentration, as given by the sand producer, is given in Table 1.

Table 1: Difference in initial concentration of alkali and hydroxyl in the crucible samples as given by the manufacturer [21]

Crucible type	Alkali	OH
A	High	Low
B	Low	High

Inductively coupled plasma mass spectrometry (ICP-MS) has been done on both of the crucible types, which confirm these concentrations. The full result on the ICP-MS, with other impurities as well, can be seen in appendix A.1.

3.2 Sample preparation

3.2.1 Crucible samples

The samples were cut both manually and by the glassblower at NTNU. For the manually cutting a coarse diamond saw was used to cut the larger pieces into smaller pieces with both the BF and the BC layer, and then a Accutom high precision saw was used to cut away the BC layer. The two saws can be seen in Figure 16.

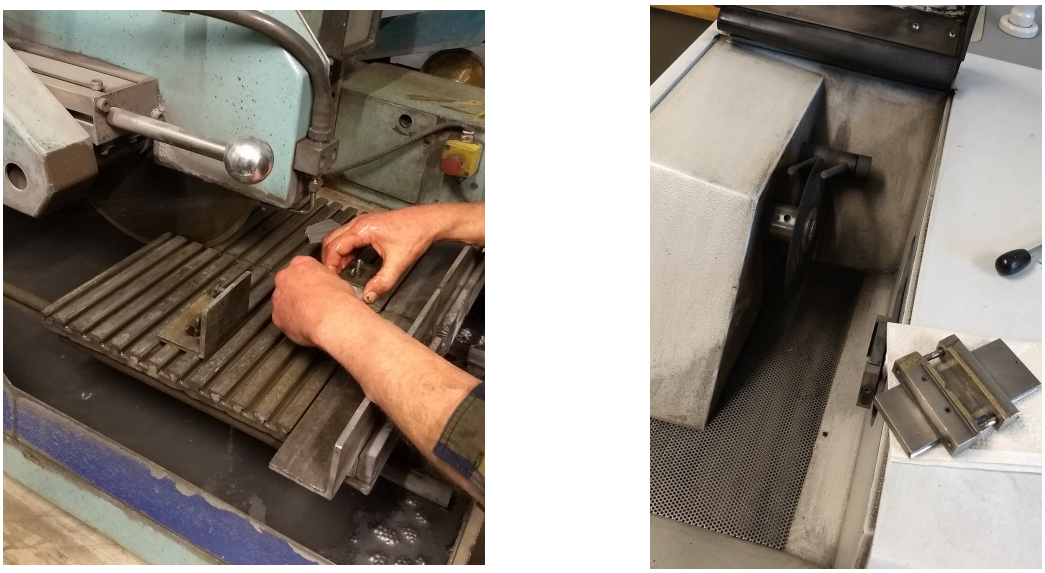

(a) (b)

Figure 16: (a) The coarse diamond saw (b) The Accutom high precision saw

The broad saw was stationary and the crucible pieces had to manually cut into the wanted size. The Accutom saw was automatic. The sample was mounted on to the saw tightly to avoid the sample from slipping during sawing, and thus breaking the sample. The final pieces were 1x1cm and 2x2cm, with a thickness of slightly above 2 mm. The final cut of both crucible types can be seen in Figure 17.

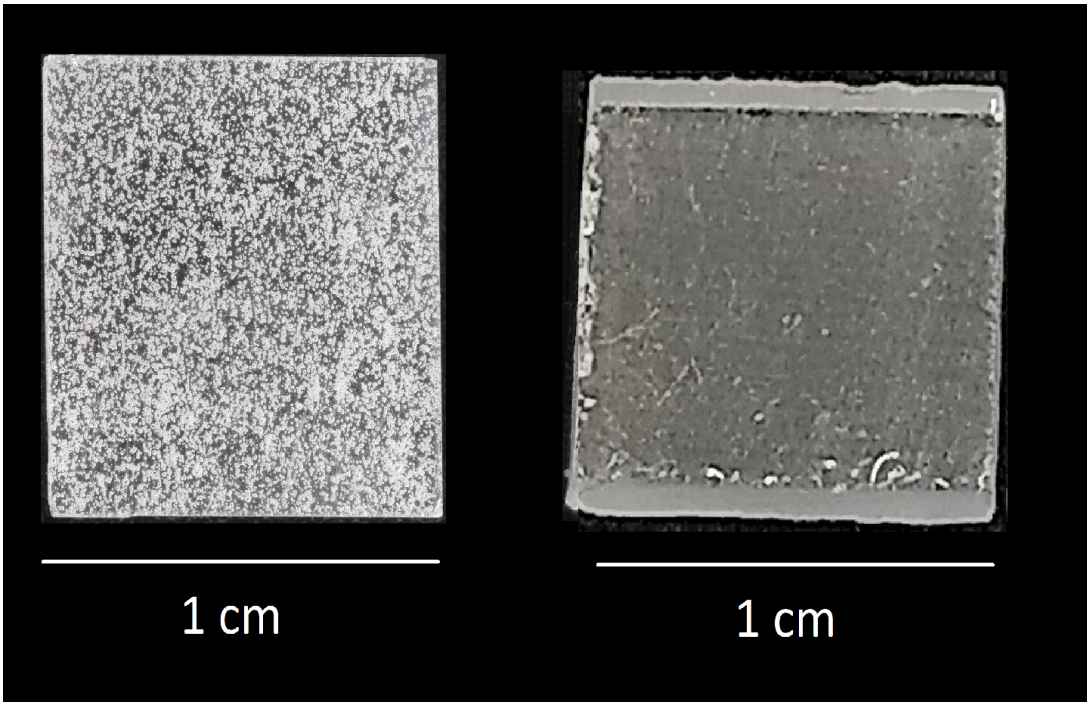

Figure 17: The final crucible cut. (a) Crucible from natural sand (b) Crucible from synthetic sand.

3.2.2 Wetting

Before the wetting experiments the samples were washed in ethanol before being inserted to the wetting furnace. This was to ensure that there were no impurities or dirt that could effect the wetting angle. The silicon used was poly silicon from Hemlock (?), and is similar that which is used in the CZ process. Lumps of the silicon was crushed with a hammer into smaller lumps with a length between 1 and 4 cm.

The small silicon pieces was then cut into even smaller pieces, and polished to make a flat surface. This can be seen in Figure 18. The flat surface is obtained to get a better grip on the silica surface, and to avoid silicon from falling off the silica when entering the wetting furnace.

The silicon reacts with the oxygen in the air and forms a silicon oxide layer, which has a higher melting temperature than pure silicon. In order to remove this layer, the silicon is placed in 10 % hydrofluoric acid for 10 minutes, and put in a beaker with ethanol for storage until needed.

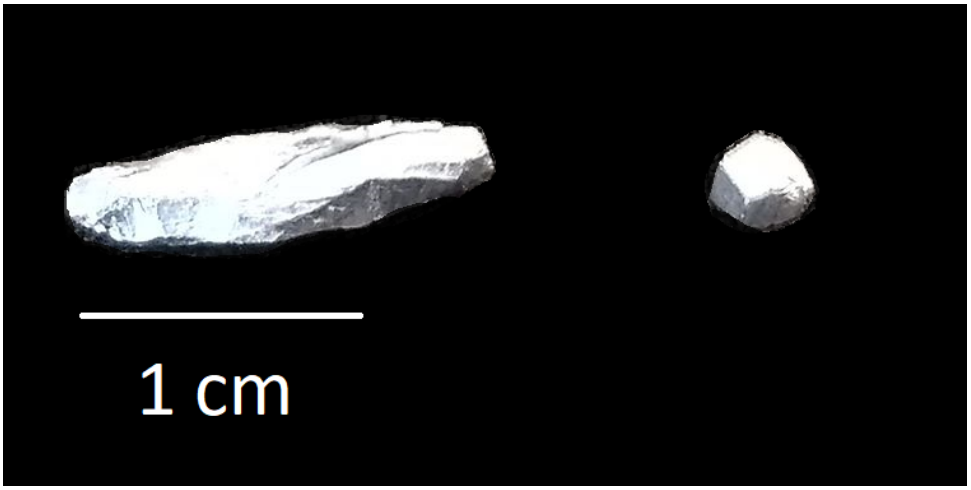

Figure 18: Left - sample as obtained from SINTEF, right - sample after cutting and polishing

3.2.3 Coating

Before coating the samples with $Ba(OH)_2$, the samples were quickly washed in destilled water and ethanol, to remove any impurities. On the heat treated silica samples, where cristobalite had been formed, the samples had been polished beforehand, to remove the cristobalite layer on the sample before being washed.

3.3 Heat treatment

As mentioned in chapter 2.1, the production method of the silica, and the sand type used, is crucial for the properties of the glass. In some types of glass the hydroxyl are removed at temperatures below 1000 ℃, where there are types where the hydroxyl concentration is nearly not effected at all at temperature above 1200 degrees [32].

3.3.1 Preliminary testing

In order to find out what temperature range the samples used in this thesis were effected, some preliminary testing had to be done, at the extremes. The preliminary tests were only done on samples made from natural quartz sand.

Sliding Flanges Tube (SFT) Furnace

For the lower limit a GSL-1500x-RTP50 tube furnace with sliding flanges was used, with a mulite tube. The samples were placed close to the end of the tube. Before running the furnace, the tube was vacuumed and filled with pure argon gas several times before running the furnace in vacuum.

The furnace can be seen in Figure 19. The tube can be moved into the heating chamber. The furnace is heated to the wanted temperature, with the tube outside the chamber. Then the tube is moved close to the heating chamber, until the temperature in the tube

reaches 300 ℃. This is to ensure longer lifetime of the tube. When the temperature reaches 300 ℃, the tube is inserted all the way, and the temperature will rise swiftly to the desired temperature. A thermocouple is placed both inside the tube and in the heating chamber, to get more accurate temperature measurement. The temperature shown inside the tube was consistently 20 ℃ lower than inside the chamber when the temperature was above 1000 ℃.

A vacuum pump was used to lower the pressure inside the tube. The pressure during the heat treatment was close to $1 \cdot 10^{-2}$ mbar, and kept at this level for the entire duration of operation when run under vacuum. When run in argon atmosphere the pressure is kept at 1 atm.

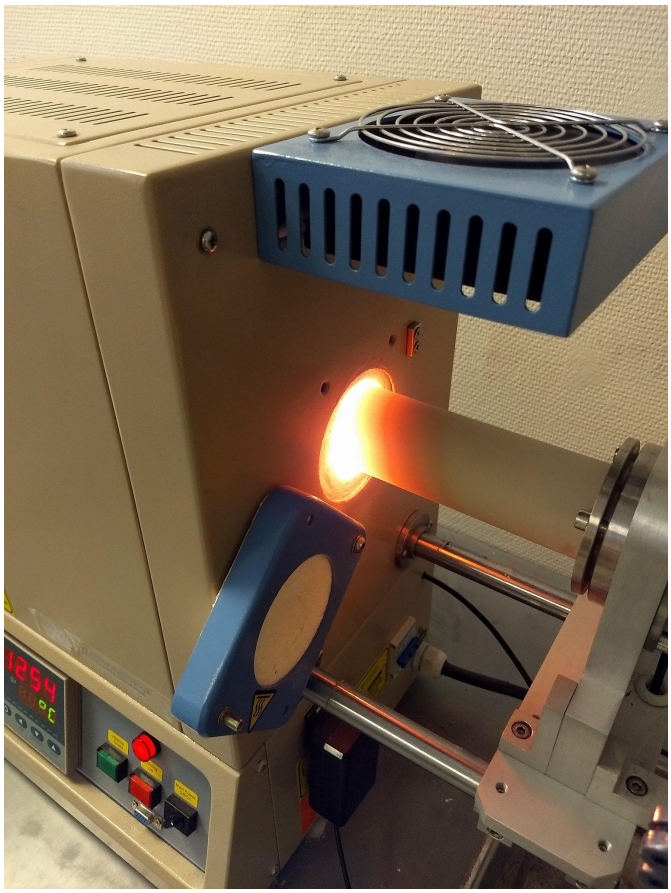

Figure 19: The SFT furnace during operation

The temperatures that were tested are given in Table 2, along with atmospheres. At 1300 ℃ an argon atmosphere was not used, due to previous low effects in this atmosphere.

Table 2: Temperatures, holding time and atmospheres for the preliminary testing.

Sample #	Temperature	Atmosphere	Time
1	1100 ℃	Vacuum	24 h
2	1100 ℃	Vacuum	48 h
3	1100 ℃	Argon	24 h
4	1200 ℃	Vacuum	24 h
5	1200 ℃	Vacuum	24 h
6	1200 ℃	Argon	24 h
7	1300 ℃	Vacuum	24 h
8	1300 ℃	Vacuum	48 h

The furnace used for these tests had a maximum temperature of 1300 ℃ when in vacuum. So in order to test higher temperature, another furnace was used.

Alumina Tube Furnace

For the higher limit an Alumina Tube Furnace was used. The samples were placed in a small graphite crucible, with a piece of molybdenum foil at the bottom, to separate the samples from the graphite. The crucible can be seen in Figure 20.

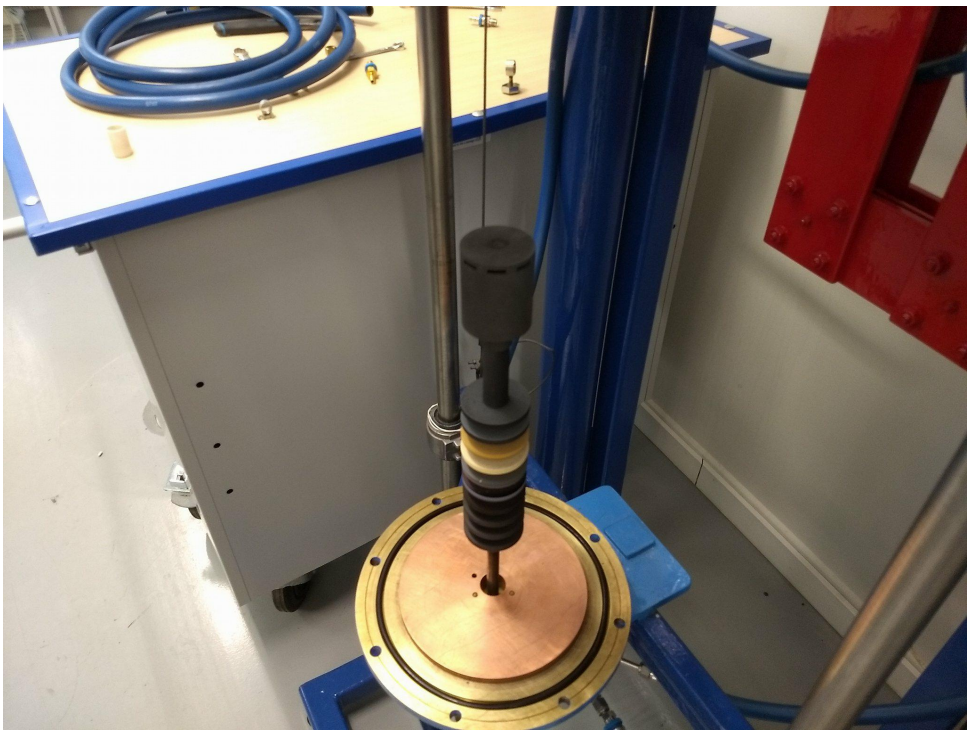

Figure 20: The alumina tube furnace in open position

Figure 20 shows the furnace in open position. After the samples were placed in the graphite crucible, the furnace was closed, vacuumed and flushed with argon three times. Figure 21 shows the furnace in closed position.

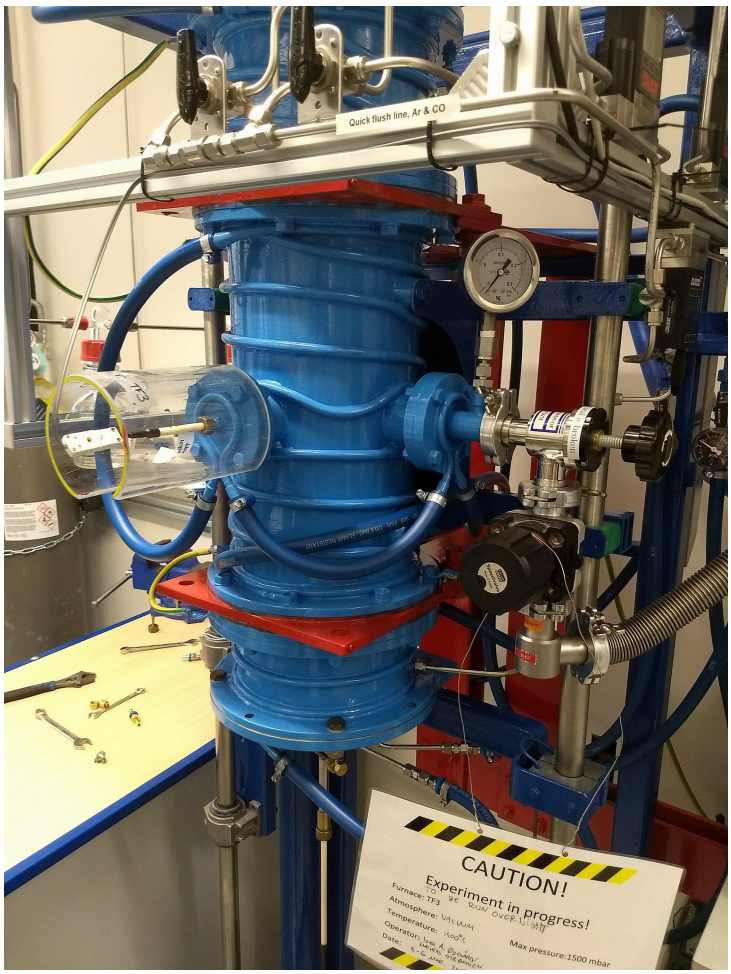

Figure 21: The alumina tube furnace in closed position.

One sample was tested on this furnace, at 1500 °C, for 24 hours, at vacuum. The pressure inside the furnace was approximately $2 \cdot 10^{-2}$ mbar during operation.

3.3.2 Main heat treatment

The furnace used for the main heat treatments was an thermal gravimetric analysis (TGA) furnace. The temperature is measured by a pyrometer, which is pointing directly into the crucible where the sample is placed. The furnace can be seen in Figure 22.

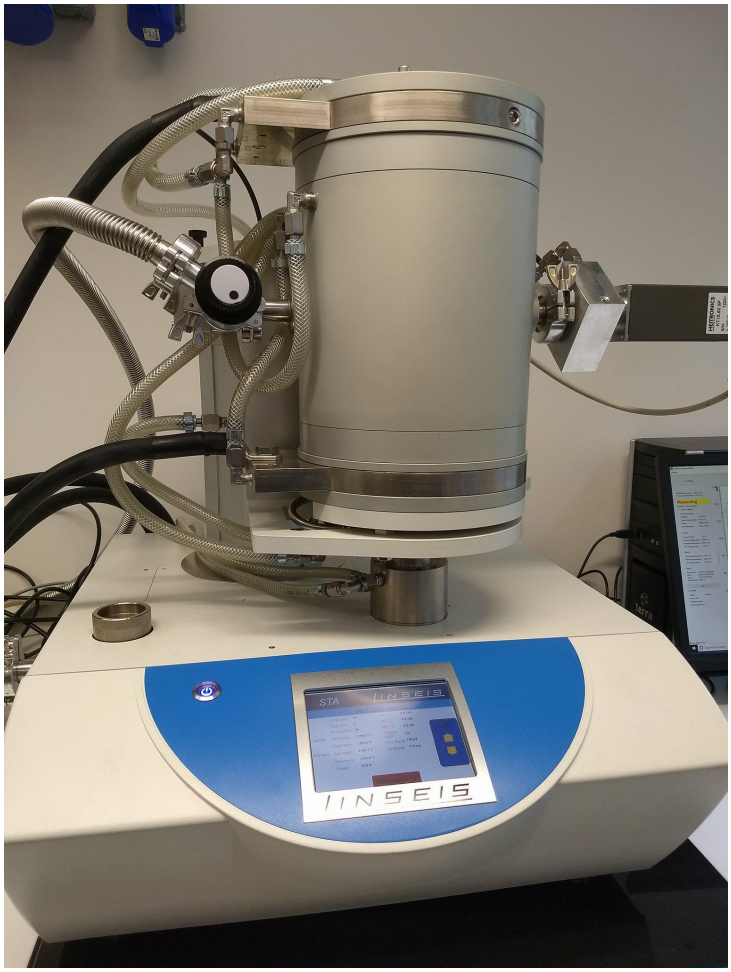

Figure 22: The TGA furnace in closed position

The furnace has a graphite heater, and a vacuum pump connected to it. Before running the furnace, the heating chamber was vacuumed and filled with argon several times in order to avoid air in the furnace, before running on vacuum during heating. The samples were placed in a graphite crucible, as can be seen in Figure 23a.

(a)

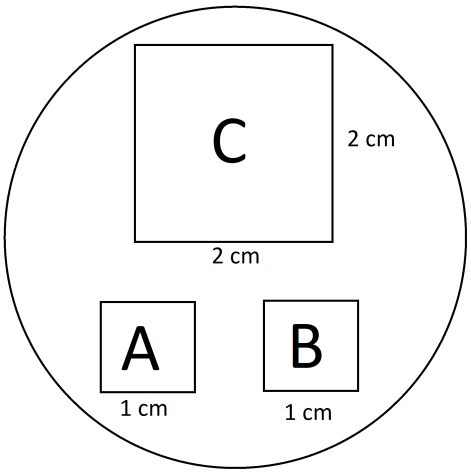

(b)

Figure 23: (a) The graphite crucible used in the TGA furnace (b) Sample placement in the graphite crucible.

Three samples were heat treated each run, one 2x2 cm, and two 1x1 cm. They were placed in the crucible as shown in Figure **??**. Samples placed in A would get tested in the wetting furnace without coating, while samples placed in B would get coated before undergoing wetting test. Sample C was a back up sample, and used to better see any structural deformations. The heating rate was 50 ℃/min untill 1100 ℃, and 20 ℃/min untill target temperature was reached.

After the preliminary testing, a matrix of temperatures, atmospheres and time was established. The parameters of the main heat treatment is shown in Table 3.As can be seen the parameters chosen regarding time and atmosphere was only 24 hours and vacuum respectively. A total of 6 heat treatments were done.

Table 3: Parameters of the main testing in the TGA furnace.

Sample type	Temperature	Atmosphere	Time
Natural	1350 ℃	Vacuum	24 h
Natural	1400 ℃	Vacuum	24 h
Natural	1450 ℃	Vacuum	24 h
Synthetic	1350 ℃	Vacuum	24 h
Synthetic	1400 ℃	Vacuum	24 h
Synthetic	1450 ℃	Vacuum	24 h

3.4 OH measurement and calculation

The FTIR spectrometer used was a Bruker Vertex 80v. The samples were placed in the sample holder with double sided tape, and placed in the compartment as shown in Figure 32.

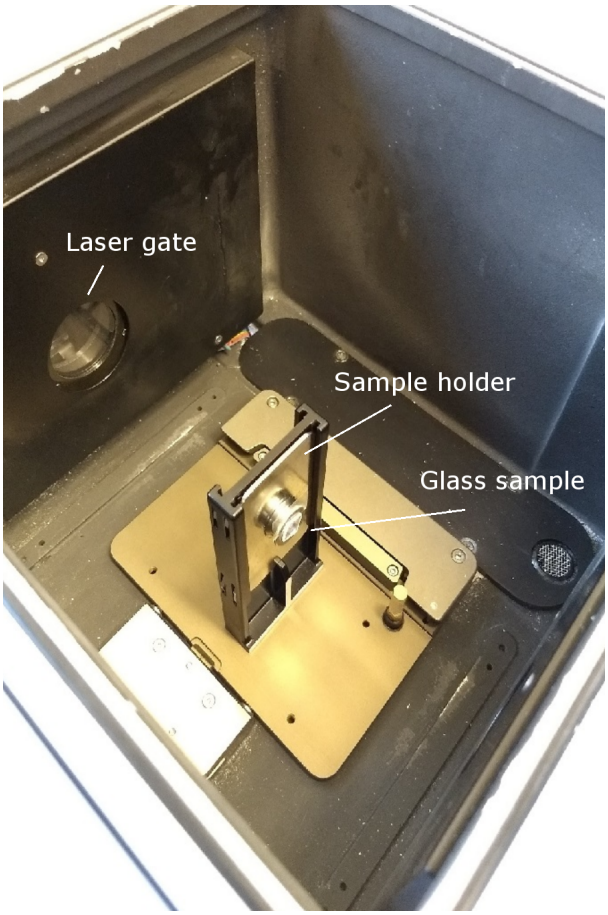

Figure 24: Open position of the FTIR spectrometer compartment.

When the sample was placed in the sample holder, the compartment was closed and evacuated to 2.02 hPa. To make sure that the results were correct, the samples were analyzed with FTIR 5 times, on different places. The positions were the samples were analyzed is shown in Figure 25.

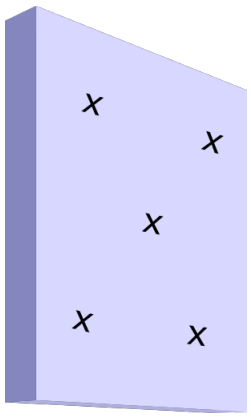

Figure 25: Positions on the samples that were analyzed.

This gave a graph of the transmission spectre for each position, which was run through a script in the programming software MatLab. The average of each sample was calculated. The procedure is described in chapter 2.8. The MatLab script that was used can be found in the Appendix A.2.

3.5 Coating

To create similar conditions as industrial crucibles, the heat treated samples were examined with and without coating. This is to investigate whether or not if the coating effects the wetting angle. Barium was used as a devitrification agent in this thesis.

The procedure followed in this thesis is motivated by an US patent and the work of a previous master student [12, 33]. From previous work done, spray coating was chosen to be easiest method, with the most similar results to industrial coating [12]. The coating was done 1-3 days before wetting experiments were done on the samples.

3.5.1 Spray coating

The solution used as coating was $Ba(OH)_2$. A saturated solution was made of $Ba(OH)_2$ and distilled water. At room temperature the solubility of $Ba(OH)_2$ is 5.14g in 100 mL water, which gives 0.28 M.

The setup is presented in chapter 2.3, and the parameters are found from a previous master thesis [12].

A spray coating machine from SONO-TEK Corp is used. The setup can be seen in Figure 26

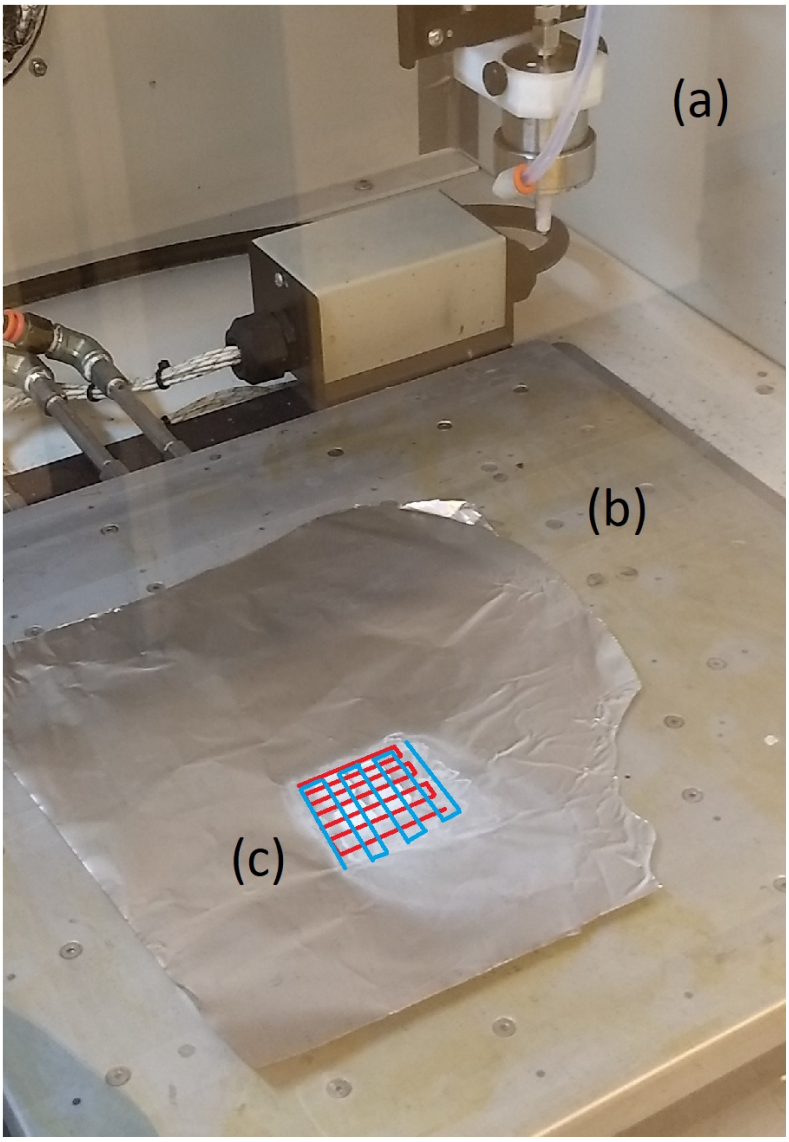

Figure 26: The machine used for spray coating. (a) the ultrasound nozzle (b) heating plate (c) alternating spray patterns (red and blue).

The saturated solution was inserted into the automatically controlled syringe. As solution carrier, nitrogen gas was used, and an ultrasound nozzle was used in order to get small enough drops. To make sure the solution would evaporated fast enough, and to make sure surface reaction, the heating element in the machine was used. It was heated to 80 ℃and the samples were pre-heated for 30 minutes before coating. The spraying pattern was done in alternating zigzag pattern, as can be seen in Figure 26. To make the coating most similar to industrial coating, the infuse rate was set to 0.7 ml/min with an area spacing of 2 mm. As the samples are relatively small, several samples were coated at the same time.

To make sure the coating was even and thick enough, the samples were coated a total of 4 times. After the coating was finished, the samples rested on the heater for another 30 minutes. To make sure the $Ba(OH)_2$ reacts with the carbon dioxide in the air, the samples are left in a fire hood over night.

Limitations

Due to movement in the sprayed coating before evaporation, the coating might not be completely homogeneously spread. The coating is also easily brushed away, and the sample must be handled with care after coating.

3.6 Wettability

Heat treated and untreated samples, coated and non-coated, were tested in a wetting furnace to find the contact angle between silicon and the sample. The wetting furnace has a camera taking pictures inside the heating chamber, and a barometer measuring the pressure. The temperature is measured by thermocouples inside the heating chamber, as well as a pyrometer pointing at the sample. The entire furnace is connected to a vacuum pump, and has available argon (6N purity) and CO as inlet gas. Water cooling is present to cool the system, and to avoid the O-rings from melting. The entire furnace can be seen in Figure 27.

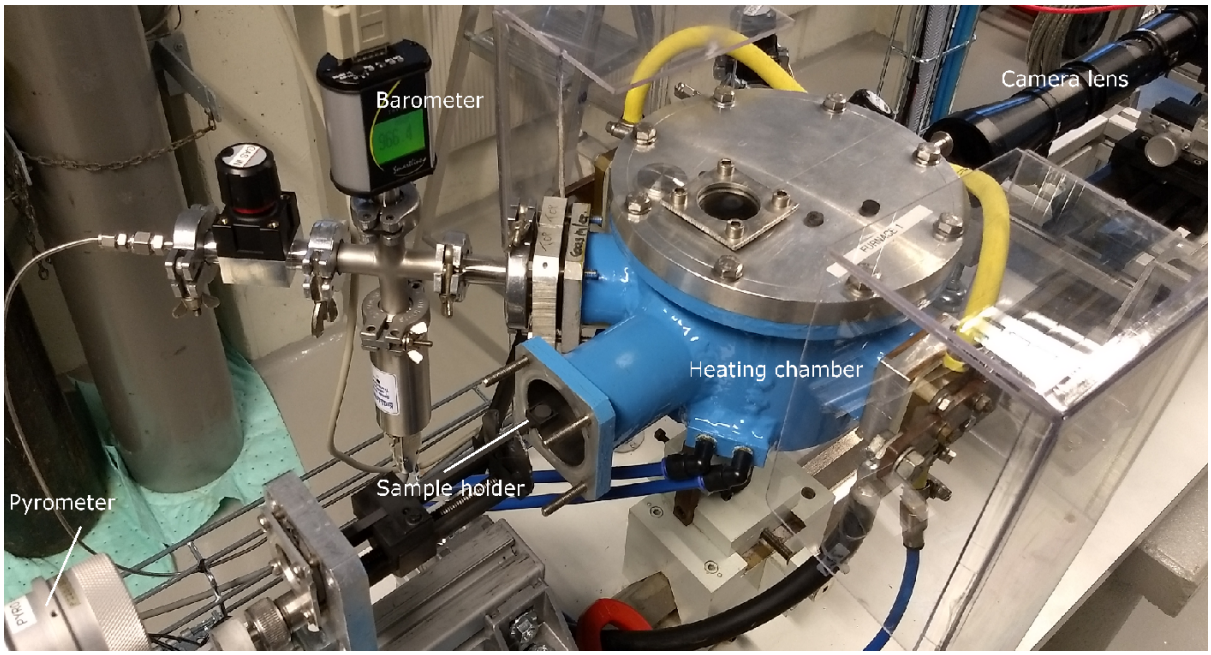

Figure 27: Wetting furnace with its components before sample is loaded and inserted.

A small lump of polysilicon was put on the silica sample as shown on Figure 28 and inserted into the furnace. The chamber was subsequently evacuated to vacuum.

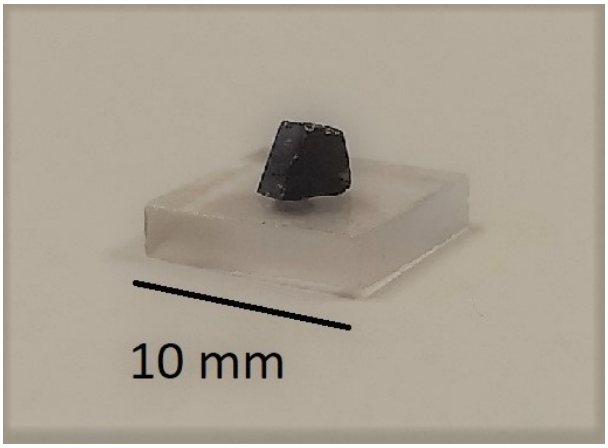

Figure 28: The polysilicon sample placed on a crucible sample.

To remove any oxide layer that had been formed on the silicon surface, the sample was placed in a 10% HF solution for 10 minutes, and then rushed to the furnace. Air was removed and an argon flow was established. The non-coated samples were heated to 1450 ℃ in 7 minutes. To prevent the oxygen from the silica glass to react with silicon, and creating a oxide layer, the whole test was performed under low pressures. During heating, a low argon flow was run through the furnace, and the pressure was kept at approximately 20 mbar. For the coated samples, the target temperature and heating rate was increased to 1470 ℃ in 6 minutes. A picture was taken every 5 seconds, and the software calculated the wetting angle for each picture. The picture with the largest wetting, preferably at the end of the experiment, was chosen.

3.7 SEM

To investigate how the coating precipitated and reacted at the surface of the samples, SEM was used. In order to get SEM images, additional preparations steps had to be performed.

The entire sample, except the region that was investigated, was covered in aluminum foil to ensure current flow. In order to get a good conductivity, the sample was coated in a very thin layer of carbon. The coating is coming from carbon that is composed in a sputtering device. A sputtering time of 8 seconds is used two times to ensure good enough covering.

3.8 Summary

In Table 4 all the different experiments done can be seen. FTIR was done on all the samples, and SEM was done on coated untreated samples.

Table 4: Summary of all experiments done in this thesis

	Heat treatment	Wetting	Coating
Natural Quartz	No	Yes	Yes
	No	Yes	No
	1350	Yes	Yes
	1350	Yes	No
	1400	Yes	Yes
	1400	Yes	No
	1450	Yes	Yes
Synthetic Quartz	No	Yes	No
	No	Yes	Yes
	1350	Yes	No
	1350	Yes	Yes
	1400	Yes	No
	1400	Yes	Yes
	1450	Yes	No
	1450	Yes	Yes
Natural Quartz Preliminary Testing	1000	No	No
	1000	No	No
	1100	No	No
	1100	No	No
	1200	No	No
	1200	No	No
	1300	No	No
	1300	No	No
	1500	No	No

4 Results

4.1 Heat treatments

4.1.1 Preliminary testing

For the lower temperature preliminary testing, as described in chapter 3.3.1, there was no visible formation of cristobalite formation on any of the samples heat treated with any of the parameters given in Table 2.

For the upper limit of 1500 ℃, the results can be seen in Figure 29.

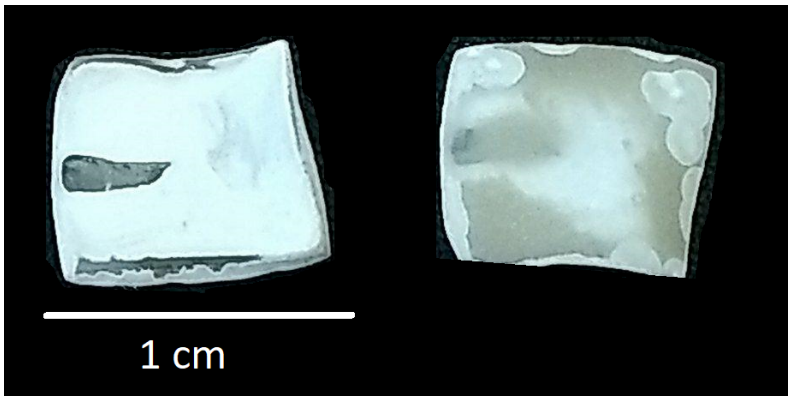

Figure 29: Natural crucible sample heat treated at 1500 ℃for 24 hours under vacuum. Front and back respectively.

As can shown in Figure 29, the sample got completely deformed. A thick cristobalite layer was formed on the front of the sample, and on the back of the sample brownish rings have started to form. The total sample also shrank significantly, with the thickness reduced to about half of its original thickness.

4.1.2 Main testing

The samples presented in this section have been heat treated as described in chapter 3.3.2. Although three samples were tested at the same time, only one of them is shown in this thesis. The samples that were heat treated together was close to identical.

Natural crucible

The natural samples that were heat treated can be seen in Figure 30.

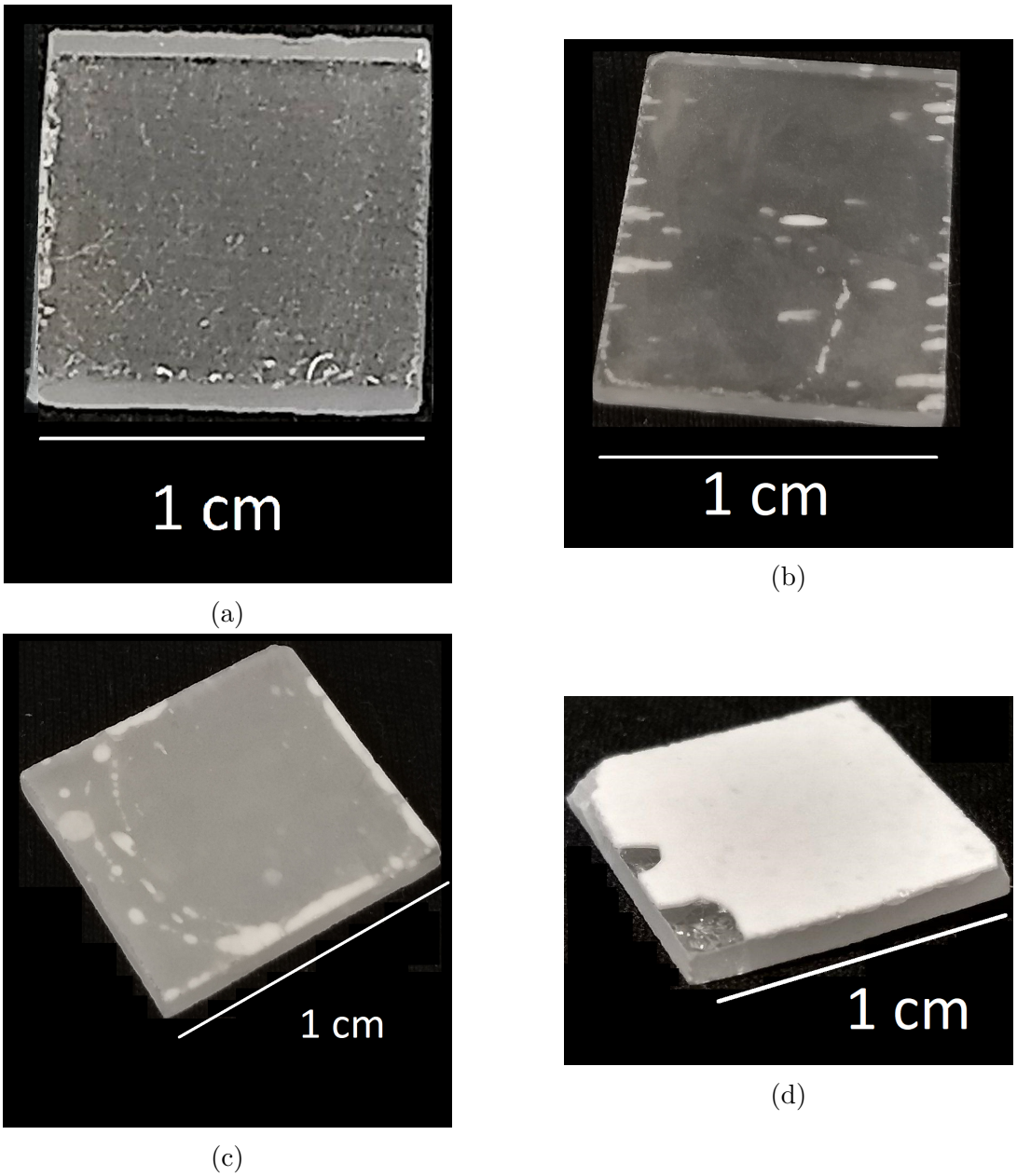

(a) (b) (c) (d)

Figure 30: Natural crucible samples. (a) No heat treatment (b) 1350 ℃ 24 hours (c) 1400 ℃ 24 hours (d) 1450 ℃ 24 hours

Some small white marks can be seen in Figure 30(a). This is cuts from the sawing, and is on the backside. The front side is completely smooth and transparent. The white spots on picture (b) and (c) is cristobalite. The amount of cristobalite in (c) is visibly greater than in (b). In picture (d) the entire surface is covered in a thick cristobalite layer.

Synthetic crucible

The synthetic samples that were heat treated can be seen in Figure 31.

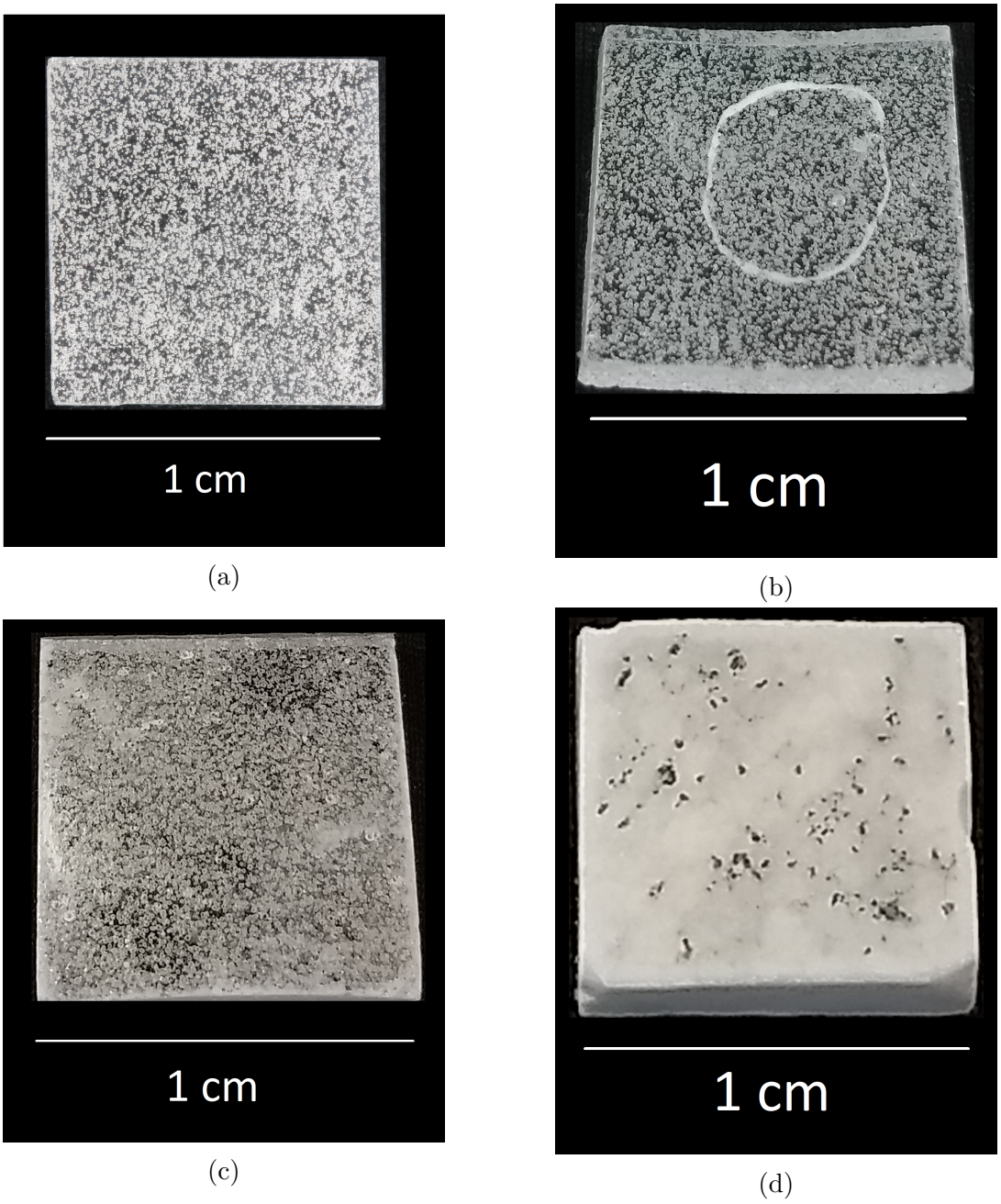

(a) (b) (c) (d)

Figure 31: Synthetic crucible samples. (a) No heat treatment (b) 1350 ℃ 24 hours (c) 1400 ℃ 24 hours (d) 1450 ℃ 24 hours

In picture (b) a white ring of cristobalite is starting to form. This was the case on all three samples heat treated at this temperature. In picture (c) a more uniform layer of cristobalite has been formed. In picture (d) the entire surface of the sample has been covered in cristobalite, with some formation of brown spots. The layer was easily broken, and flakes fell of.

4.2 FTIR results

4.2.1 Untreated samples

The FTIR - results for the untreated samples can be seen in Figure 32. Only one of the plots of each of the samples is shown, due to low variate. The remaining plots can be seen in Appendix A.3.

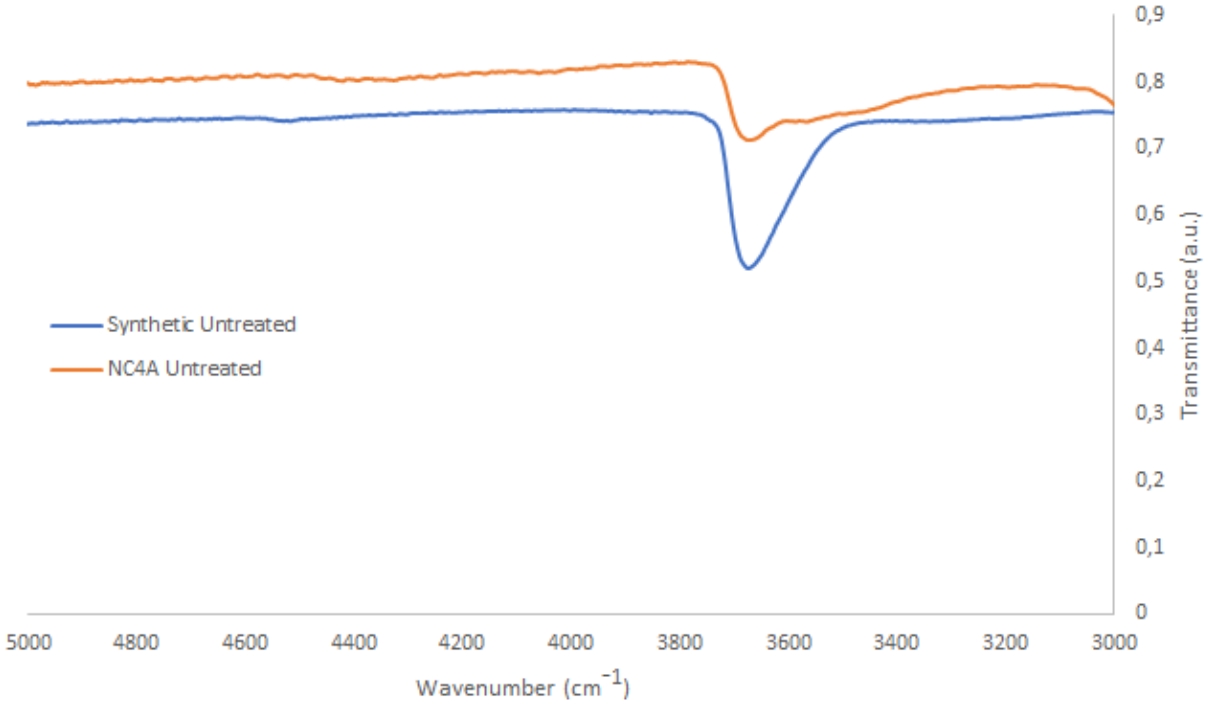

Figure 32: The transmittance of untreated synthetic (blue) and natural (orange) crucibles at different wavenumbers.

For both graphs, the peak at around 3650 cm^{-1} is clearly visible, with different peak heights. From the method explained in chapter 3.4, the OH concentrations were obtained. They can be seen in Table 5. As multiple tests were done, a standard deviation was also calculated.

This will be the only transmittance/wavenumber plot that will be shown in this thesis. All other plots will be given in the appendix. All plots have similar curves, and is of no interest when the OH concentration has been calculated. The OH concentrations coincides with the concentrations given by the manufacturer in chapter 3.1.

The FTIR results were obtained by using the method described in chapter 3.4.

4.2.2 Preliminary testing

The OH content in the samples that were run in Argon atmosphere in the slide tube furnace were not effected by the heat treatment. The samples that were run in vacuum had a reduction in OH content between 1 and 13 ppm OH, in the sample heat treated at 1000 ℃ and 1300 ℃ respectively. The other samples had a varying OH content between these values. There was no significant difference in OH content in the samples that were heat treated for 24 hours as opposed to 48 hours at these temperatures.

The OH content deformed samples that were heat treated in the ATF could not be measured. The transmittance in the sample was low, and the spectrum was not similar to the characteristic silica spectrum.

4.2.3 Main testing

The OH content calculated from the main testing can be seen in Table 5.

Table 5: Measured OH contents with uncertainties

Natural Crucible	OH content (ppm)	Uncertainty (ppm)
No heat treatment	50.3	pm 2
1350	35.5	pm 0.5
1400	36.8	pm 0.4
1450	31.8	pm 2.5

Synthetic Crucible	OH content (ppm)	Uncertainty (ppm)
No heat treatment	99.3	pm 7
1350	44.5	pm 2.3
1400	31.75	pm 1.5
1450	NA	NA

Each sample was analyzed 5 times in the FTIR, as previously described. For some of the runs, the spectrum did not follow the characteristic spectrum for silica. Those spectrum was not included in the OH-calculation. This left between 5 and 3 graphs to calculate the average OH content. For the sample made from the synthetic crucible that was heat treated at 1450 ℃, for 24 hours, no transmittance spectrum was possible to obtain. Graphs of all the spectra can be found in Appendix A.3.

4.3 Wetting

4.3.1 Natural non-coated samples

For all the wetting experiments done on natural non-coated samples the silicon melted completely. However, when sample (d) melted it drifted towards the edge, and to avoid the sample from falling of the substrate, the experiment had to be stopped after 6 minutes and 30 seconds. For the other samples the wetting furnace was shut down 15 minutes after melting. The melted silicon on the samples can be seen in Figure 33, with the respective wetting angle, θ.

(a) No heat treatment, $\theta = 88.08°$

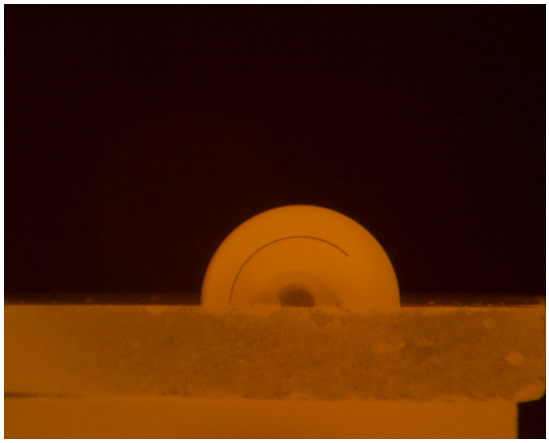

(b) Heat treated at 1350 ℃ 24 hours, $\theta = 88.64°$

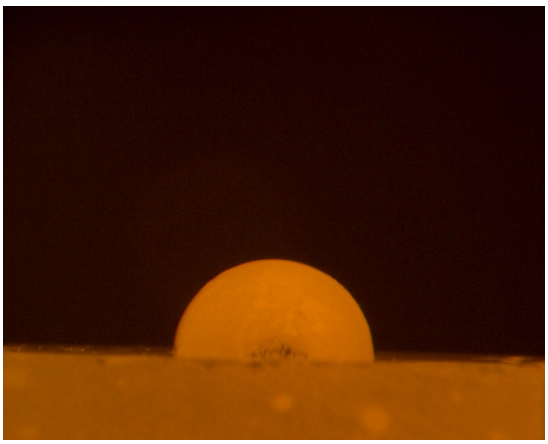

(c) Heat treated at 1400 ℃ 24 hours, $\theta = 89.84°$

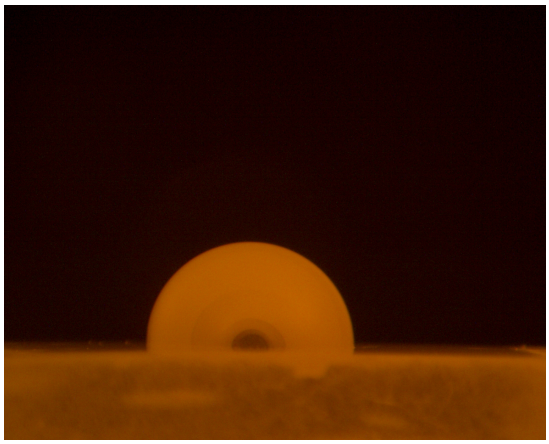

(d) Heat treated at 1450 ℃ 24 hours, $\theta = 93.40°$

Figure 33: Non-coated natural crucible sample with melted Si on top.

The wetting angles for the sample with no heat treatment, the sample heat treated at 1350 ℃ for 24 hours, the sample heat treated at 1400 ℃ and the sample heat treated at 1450 ℃ were 88.08°, 88.64°, 89.84° and 93.4° respectively. The wetting angles (θ) plotted against the heat treatment done on each sample can be seen in Figure 34 along with their respective OH content.

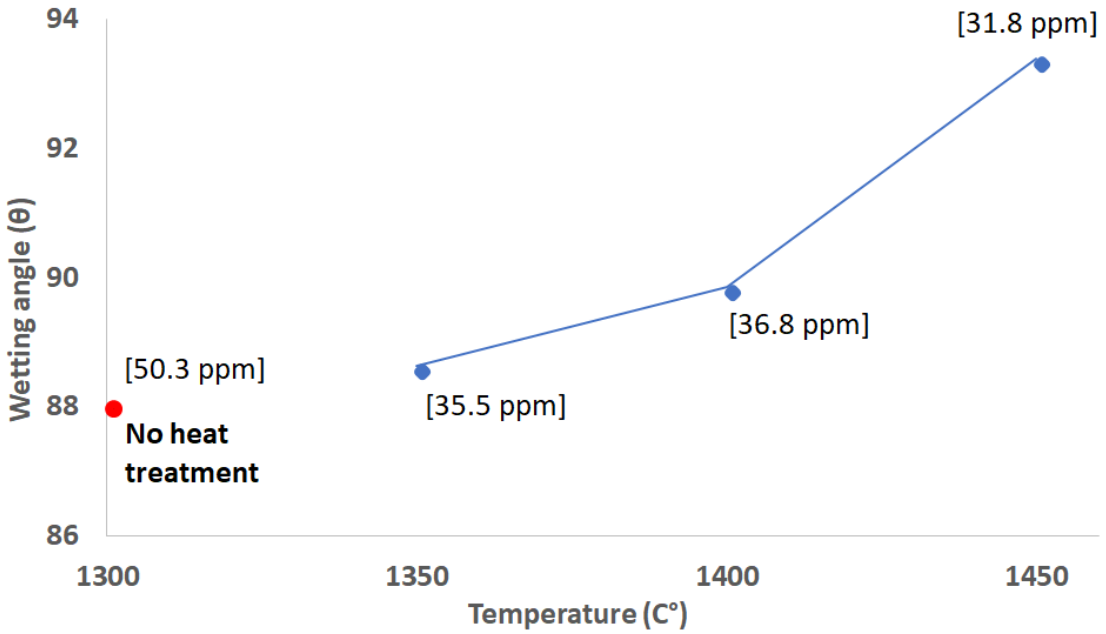

Figure 34: Wetting angle for natural non-coated samples with different heat treatment temperature done on the crucible piece, with the respective OH content.

As can be seen in Figure 34, the wetting angle increases with increased temperature of heat treatment.

4.3.2 Natural coated samples

The coated sample did not melt completely. The results can be seen in Figure 35. On Figure 35a, on the left side of the silicon, a small edge can bee seen, reaching all the way down to the sample. In the middle of the silicon, a small, dark spot can also be seen. This is silicon oxide, which has not melted. The sample on Figure 35b did almost completely melt, however the silicon oxide layer can be seen in the centre, and at the left "three phase" point. The silicon on Figure 35c had a oxide layer on the top, however, close to the silica substrate, the sample was completely melted. An oxide layer is also present in Figure 35d. Despite an oxide layer forming, the silicon did melt, and it was possible to measure a wetting angle.

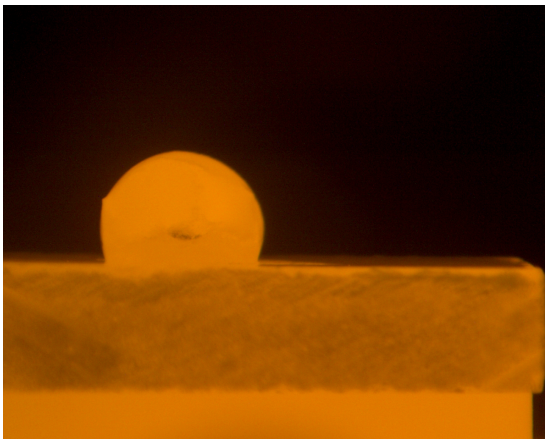

(a) No heat treatment, $\theta = 111.78°$

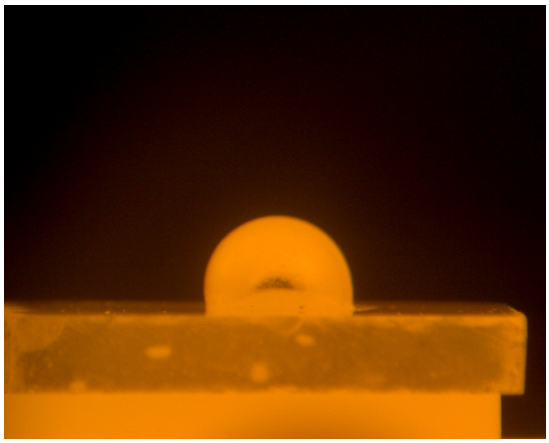

(b) Heat treated at 1350 ℃ 24 hours, $\theta = 103.96°$

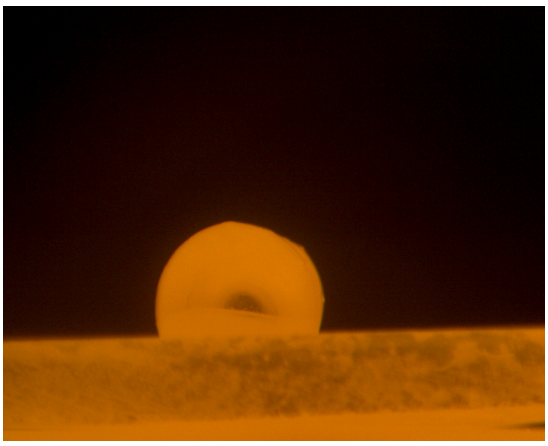

(c) Heat treated at 1400 ℃ 24 hours, $\theta = 108.51°$

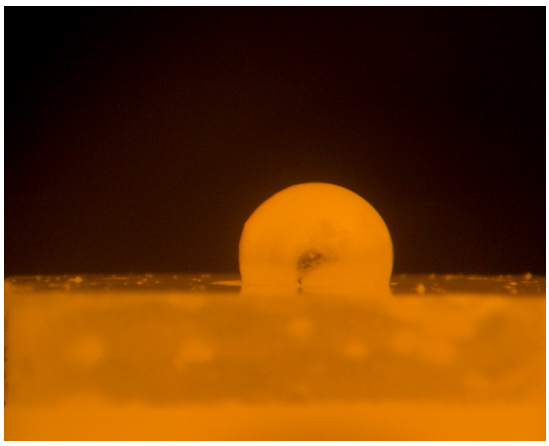

(d) Heat treated at 1450 ℃ 24 hours, $\theta = 109.20°$

Figure 35: Coated natural crucible sample with melted Si on top.

The sample with no heat treatment had a wetting angle greater then all the other. The wetting angles for the sample with no heat treatment, the sample heat treated at 1350 ℃ for 24 hours, the sample heat treated at 1400 ℃ and the sample heat treated at 1450 ℃ were 111.78°, 103.96°, 108.51° and 109.2° respectively. The wetting angles (θ) plotted

against the heat treatment done on each sample can be seen in Figure 36 along with their respective OH content.

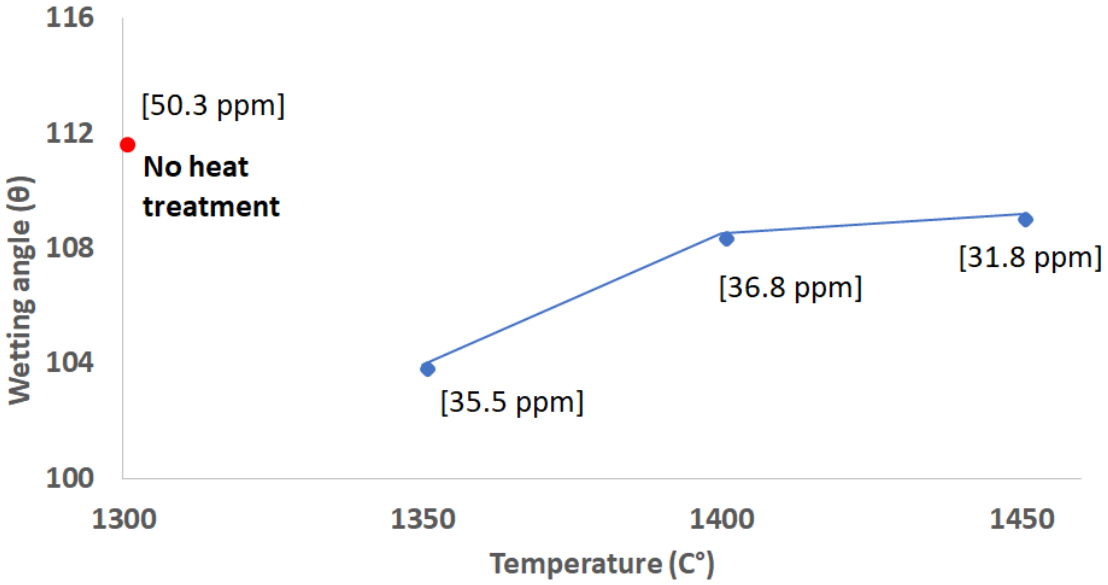

Figure 36: Wetting angle for natural coated samples with different heat treatment temperature done on the crucible piece, with the respective OH content.

All the wetting angles found on the coated samples are significantly higher than those found on the non-coated sample. The wetting angle on the non-coated samples are within the range of 88 to 94, while the coated samples are within a 104 to 112 range.

4.3.3 Synthetic non-coated samples

Each of the experiments the silicon melted completely, without any visible oxide layer. The melted silicon on the samples can be seen in Figure 37, with the respective wetting angle, θ.

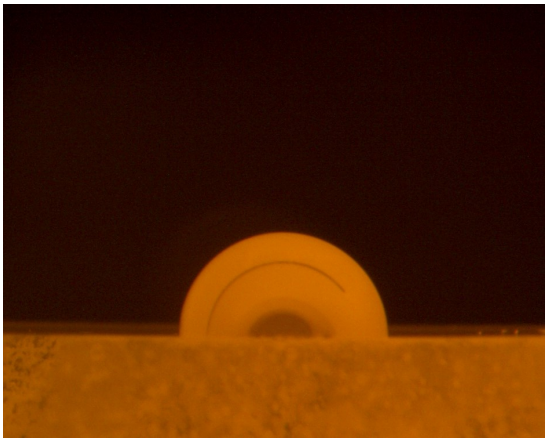

(a) No heat treatment, $\theta = 89.42°$

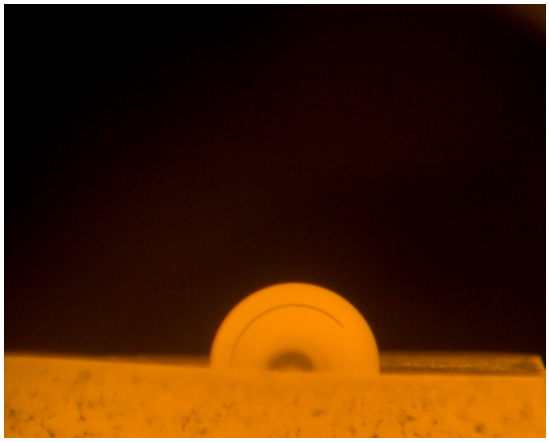

(b) 1350 ℃ 24 hours, $\theta = 92.52°$

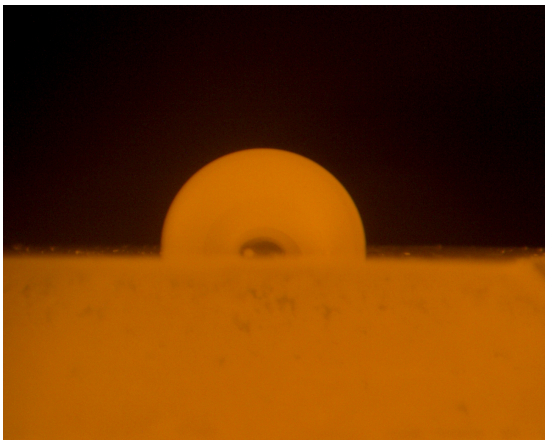

(c) 1400 ℃ 24 hour, $\theta = 93.91°$

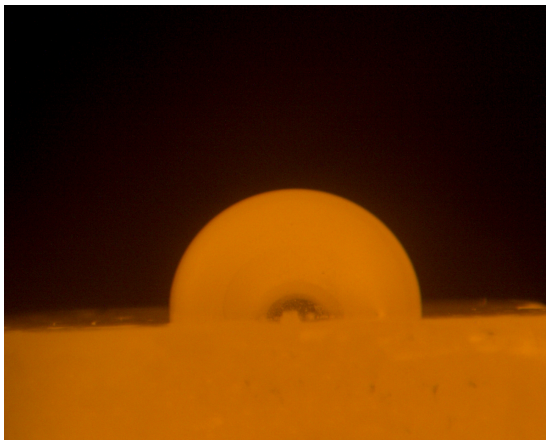

(d) 1450 ℃ 24 hours, $\theta = 93.95°$

Figure 37: Non-coated synthetic crucible sample with melted Si on top.

The wetting angle on the sample increases with higher heat treatment done on the sample. The wetting angles for the sample with no heat treatment, the sample heat treated at 1350 ℃ for 24 hours, the sample heat treated at 1400 ℃ and the sample heat treated at 1450 ℃ were 89.42°, 92.52°, 93.91° and 93.95° respectively. The wetting angles (θ) plotted against the heat treatment done on each sample can be seen in Figure 38 along with their respective OH content.

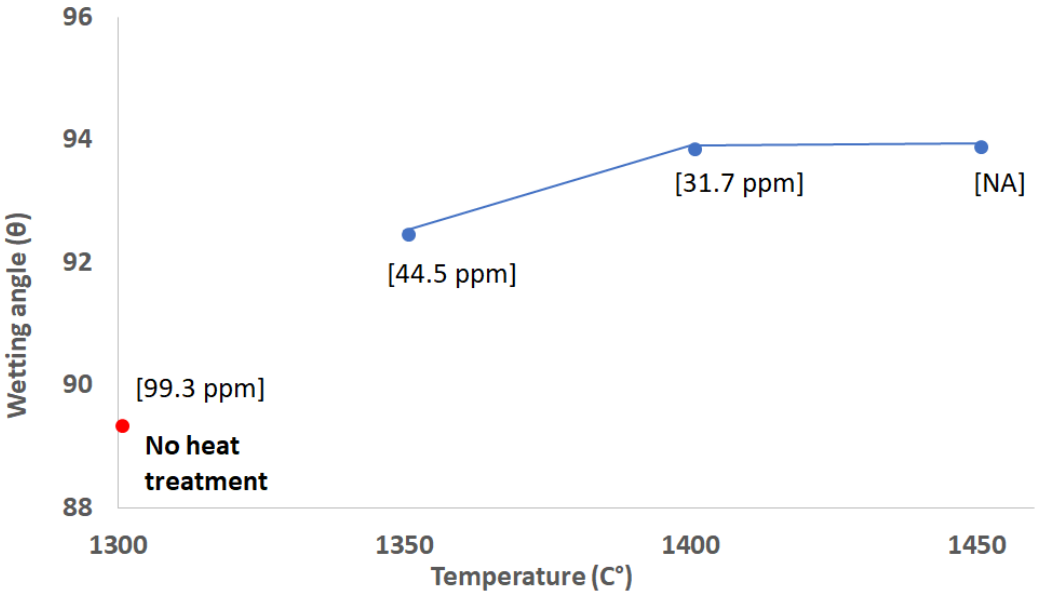

Figure 38: Wetting angle for synthetic non-coated samples with different heat treatment temperature done on the crucible piece, with the respective OH content.

4.3.4 Synthetic coated samples

The coated synthetic samples did not melt completely. This can be seen in Figure 37. On Figure 39a, an oxide layer can be seen on the lower left side area of the melted silicon, while on Figure 39b the is not completely melted at the upper left area, and is flat in this area. In lower area of Figure 39c an oxide layer can also be spotted, as well as in the center of the sample. In the Figure 39d the entire left side of the melted sample is flat, and did not melt completely.

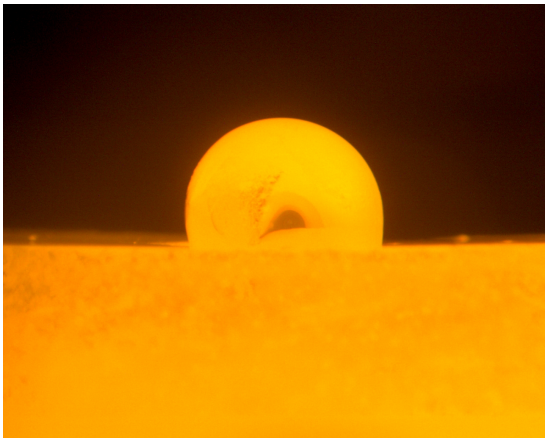

(a) No heat treatment, $\theta = 107.12°$

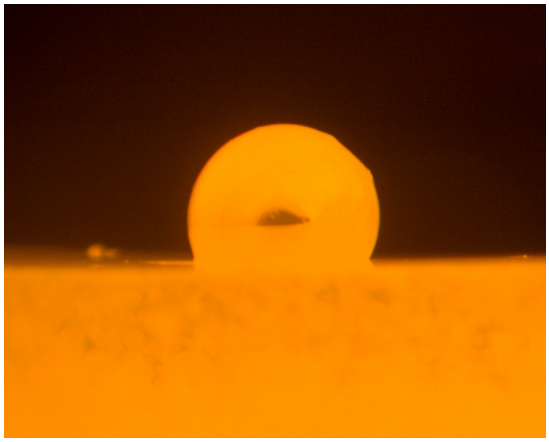

(b) 1350 ℃ 24 hours, $\theta = 115.98°$

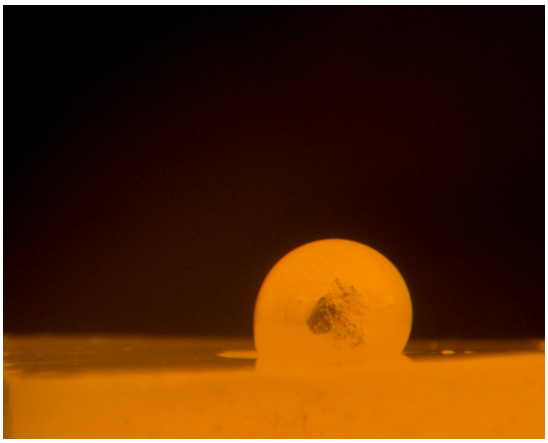

(c) 1400 ℃ 24 hour, $\theta = 117.35°$

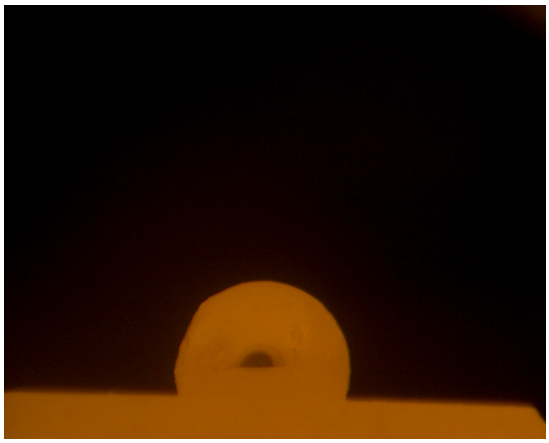

(d) 1450 ℃ 24 hours, $\theta = 110.52°$

Figure 39: Coated synthetic crucible sample with melted Si on top.

On all the samples, at least one of the sides were completely melted, from the cameras point of view, and thus the wetting angle could be measured. The wetting angles for the sample with no heat treatment, the sample heat treated at 1350 ℃ for 24 hours, the sample heat treated at 1400 ℃ and the sample heat treated at 1450 ℃ is 107.12°, 115.98°, 117.35° and 110.52° respectively. The wetting angles (θ) plotted against the heat treatment done on each sample can be seen in Figure 40 along with their respective OH content.

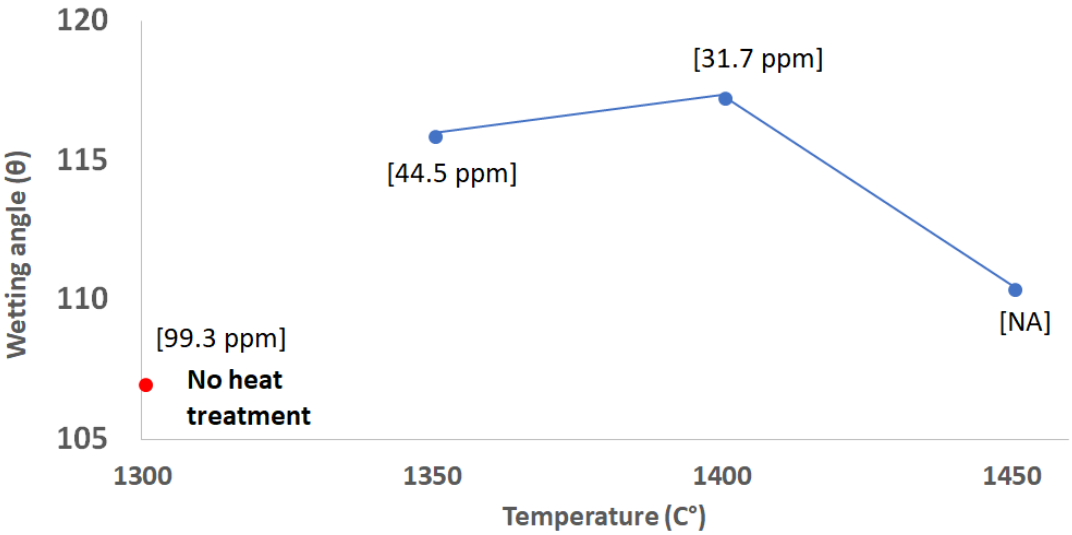

Figure 40: Wetting angle for synthetic coated samples with different heat treatment temperature done on the crucible piece, with the respective OH content.

The general wetting angle for the coated synthetic samples is between 107°and 117°.

4.3.5 Summary

The wetting angles versus heat treatments are plotted together in Figure 41.

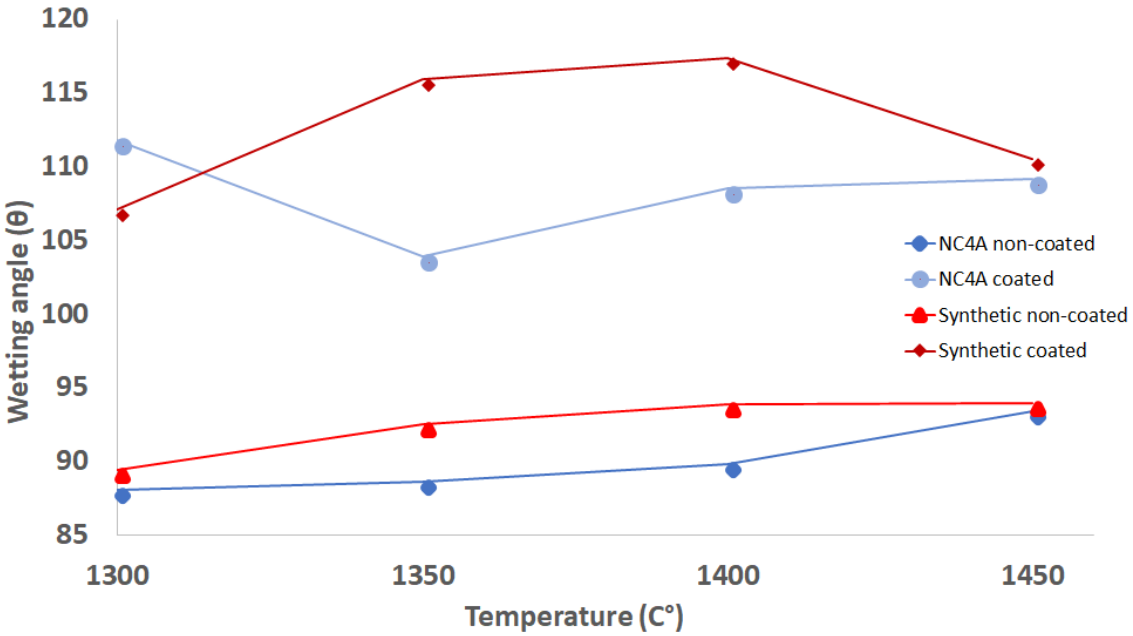

Figure 41: Wetting angle for synthetic coated samples with different heat treatment temperature done on the crucible piece.

4.4 Coating

The coating was done as described in Chapter 3.5. A sample from the synthetic crucible which has been coated is shown in Figure 42. Every coated sample have similar surface patterns as shown.

Figure 42: Silica crucible sample coated with $Ba(OH)_2$ solution

As the solution evaporated, the $Ba(OH)_2$ precipitated on the surface of the silica sample. The coating is powder-like, and easily removed when in contact with other surfaces. The coating thickness was between 0.05 and 0.01 mm on the samples.

The SEM images of a coated sample can be seen in Figure 43, at 150x magnification and 600x magnification respectively.

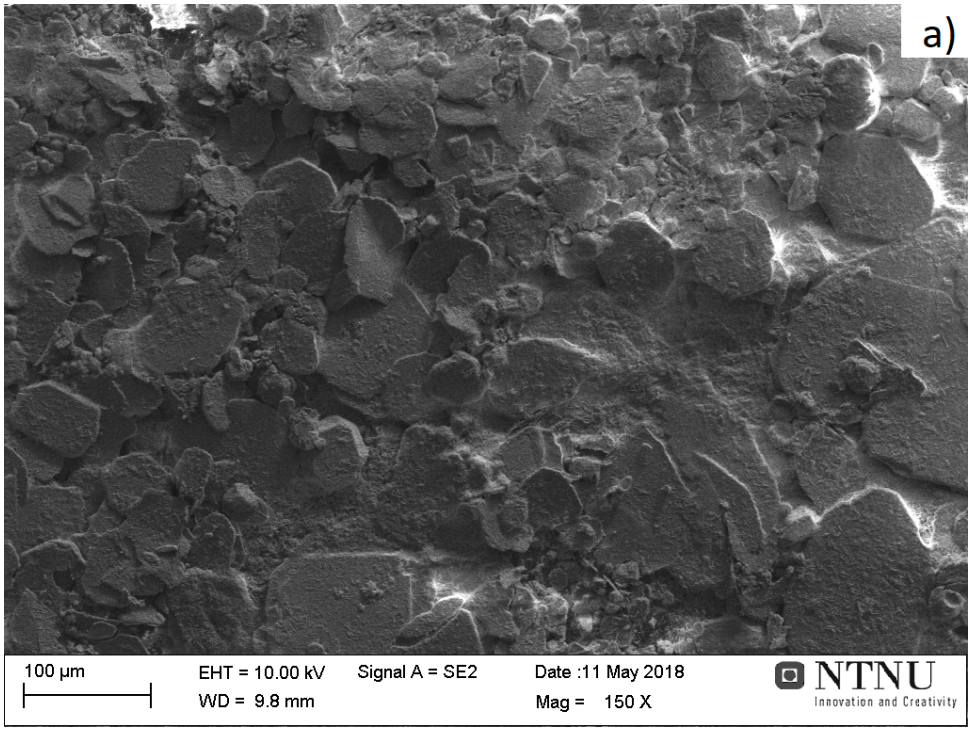

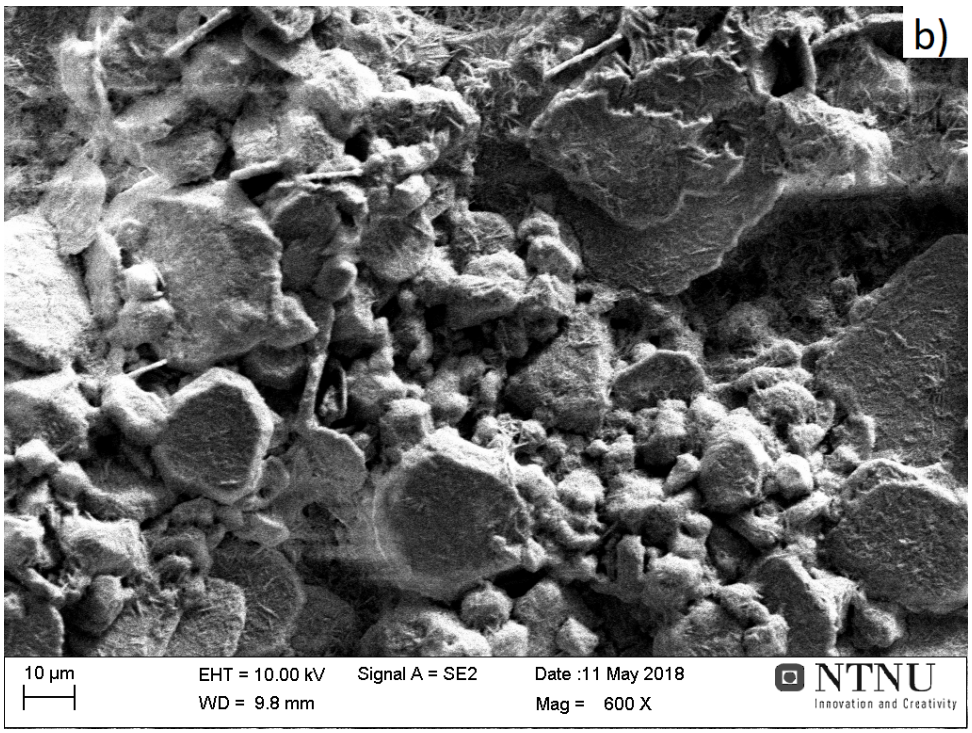

Figure 43: SEM Images of a spray coated sample at magnifications of 150x (a) and 600x (b). The flakes seen are precipitated coating.

In Figure 43a the precipitated barium coating can bee seen as flakes. The flakes are thick, and is covering the entire surface. In Figure 43b the precipitated coating can bee seen at greater magnification.

After completed wetting experiments, which lasts 15 minutes at temperatures described in chapter 3.6, a thick uniform layer of cristobalite is formed on the coated samples. On the non-coated samples, no visible amount of cristobalite can be seen. A non-coated and coated synthetic sample, with no heat treatment, can be seen in Figure 44.

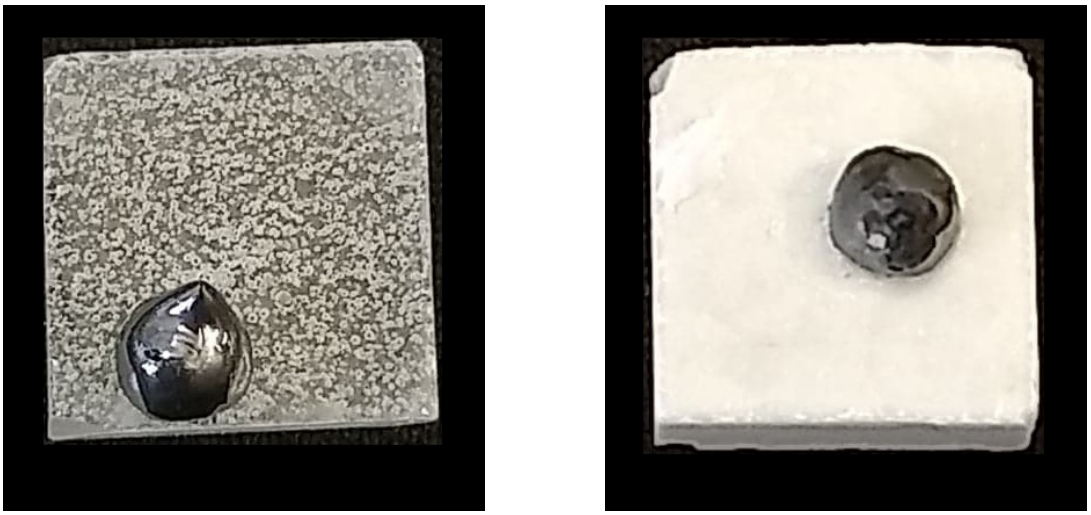

(a) (b)

Figure 44: A non-coated (a) and a coated (b) synthetic crucible sample after wetting experiment.

The cristobalite layer on the coated sample was between 0.1 and 0.2 mm thick, while a cristobalite layer on the non-coated sample did not form.

5 Discussion

5.1 Heat treatments

5.1.1 Preliminary testing

The temperature ranges for the lower limit testing was chosen based on previous work done by the author [32], where temperatures from 800 ℃ to 1000 ℃ were examined. Tubes made from a sand producer is heat treated at 1040 ℃ for 40 hours under vacuum to remove 99 % of the OH content in tubes with a thickness of 1 mm [21]. Similar starting conditions were chosen in this experiment. Heat treatments done with Argon atmosphere had lower rates of OH removal then heat treatments done under vacuum. When reaching the maximum temperature for the sliding tube furnace, some OH removal could be measured, and a thin cristobalite layer could be observed. The 1350 ℃ limit for the main testing was chosen due to these factors. The OH content in the samples heat treated 24 hours and 48 hours are almost identical. The sliding tube furnace had two thermocouples, one inside the tube, and one in the heating chamber. These temperatures coincided for all the tests, with the inner temperature 20 ℃ lower then the outer. The samples was placed on the same spot in the tube, and thus making the temperature gradient inside the tube similar for all the samples. The pressure inside the furnace was similar during the tests, with difference in pressure betwwen 2-3 Pa. The mullite tube used for these heat treatments were fresh out of the box, and it was only used for this project. This excluded any contamination from other experiments done in the furnace by others. Being able to control all these factors, the reproducibility for these experiments should be high.

The temperature for the higher limit was chosen due to the phase diagram shown in Figure 1, to see how much cristobalite would form. As seen in Figure 29, the entire sample was completely deformed, and there would be no point in increasing the temperature. The holding temperature during the CZ process is 1450 ℃, and this was chosen as the upper limit for the main testing. To measure the temperature in the furnace one thermocouple and on pyrometer was used. The thermocouple was placed right over the graphite crucible were the samples were, and the pyrometer was pointing directly at the graphite crucible. The temperature difference between these two was less than 2 ℃. As the experiment in the ATF was only done once, it is difficult to say something about the reproducibility when it comes to pressure. The furnace was also done by other people, which may have left some contamination. Preferably the main testing should also have been done in the same furnace as the preliminary tests, but due to some unwanted reaction on the thermocouple at vacuum, causing it to melt, an other furnace had to be used for the main testing.

5.2 Main testing

The main heat treatments for this project was done in the TGA furnace. For all the samples the holding time at the operating temperature was 24 hours. This was done based on the results in the preliminary testing, and from literature, where most of the OH content was removed early on in the heat treatment [20]. The furnace could only be used during working hours. Thus, in order to get more than 2 experiments each week, 24 hours was a proper duration. To measure the temperature in the TGA furnace, a

pyrometer was attached. The pyrometer was pointing on the crucible where the samples were. The samples were placed in the same position in the crucible on each run, as seen in Figure 23b. If any significant temperature gradient exists in the crucible, all the samples that were coated had been through the same temperature, and equally with the non-coated samples, by being placed in the same position in the gradient. The pressure for each run was identical, and was between 0.5-2 Pa. All the runs were done after each other, therefore any impurities that was in the furnace would effect every sample equally. Due to the parameters being so similar, and controllable, the experiment has good reproducibility.

5.2.1 Natural samples

The amount of cristobalite that forms is visibly increasing, as can be seen in Figure 30. The difference in amount between Figure 30b at 1350 ℃ and Figure 30c ℃, but when the temperature increases to 1450 ℃, the amount increases significantly. The cristobalite layer for this sample is thick, and is easily peeled of. If this heat treatment was done on a crucible as pretreatment before stacking with silicon, the amount of cristobalite woulde make it not suited. Flakes may fall of during feedstock loading, and cause damages to the silicon crystal. At approximately 200 ℃ the cristobalite will expand at a different rate than silica, as described in chapter 2.1. This will cause the cristobalite layer to crack and become unstable.

5.2.2 Synthetic samples

The synthetic samples have a similar reaction to the heat treatment as the natural samples. In Figure 31b a white ring is clearly forming, and as the temperature of the heat treatment is increasing, the layer is getting more homogeneously, as can be seen in Figure 31c. When heat treated at even higher temperatures, the sample is completely covered in a thick layer of cristobalite, with brownish spot starting to form, as can be seen in Figure 31d. A CZ-crucible will with this amount of cristobalite have the same problems as mentioned for the natural crucibles. If a crucible is going to be heat treated before use, this should be done at temperatures below 1450 ℃, in order to avoid the thick cristobalite layer.

5.2.3 OH content

From Table 5, the OH content is clearly reduced for both crucible types, and heat treatment is working to remove OH from silica, as expected. For the natural crucible the OH content is reduced by less then half, and about one third for the synthetic crucible. However, it does not go below 30 ppm for either of them. More experiments should be done in the future, with longer holding time, to investigate if there is a threshold for these types of crucibles. It was not possible to measure the OH content in the sample in Figure 31d, due to no transmittance. This was probably due to the fact that the synthetic samples had a lot more bubbles in the BF layer, and cristobalite has formed on the inner surface of these bubbles, thus blocking the IR light from penetrating the sample. From Table 5 it can be assumed that it is slightly lower than the previous samples. It is not given that cristobalite has formed in the other samples, thus effecting the FTIR results by blocking

the IR light. By taking 3-5 FTIR spectra for each sample, and orienting the samples to avoid the IR light to hit the white spots, the probability of the blocking of light is severely reduced. The uncertainties can be seen in Table 5, and were found by using a standard deviation formula [34]. Both crucible types had a low deviation when heat treated at 1350 ℃ and 1400 ℃. The natural sample heat treated at 1450 ℃ had an increase in uncertainty, which may be because of poor polishing and formation of cristobalite inside the sample. The uncertainty in general is low, and the OH content can be considered accurate.

5.3 Wetting

5.3.1 Non-coated samples

As it can be seen in Figure 34 and Figure 38 the wetting angle is increasing with increased heat treatment, and thus increasing with lower OH content. This shows that by reducing the OH content, the reactivity between silicon and silica is reduced. For the non-coated samples, the silicon melted easily, and a wetting angle was easily obtained. The pulsating effect described at the end of chapter 2.6 was not very noticeable, and the drop size was more or less consistent, and the highest angle for each sample was used as the wetting angle, and towards the end of the experiment. For the sample in Figure 35d the duration where it was melted was shorter than the other, which may effect the wetting angle. According to theory, the wetting angle will stabilize after some time, and when this sample was not melted for as long as the others, this is something that has to be considered.

5.3.2 Coated samples

Silicon on the coated samples did not behave the same way as on the non-coated samples. There is no clear trend in the wetting angle, compared to the non-coated samples. An oxide layer formed on the surface of the silicon during heating, and did not completely disappear when the silicon melted. This can clearly be seen in Figure **??** and in Figure 39. This affects the wetting angle, and can be seen for instance in Figure **??**a, where the non-melted oxide layer on the left side makes a different angle than the more melted right side. This effect can also be seen in Figure 39a. The pulsating effect is also more significant in these experiments. During the melting process it could be observed that the oxide layer periodically evaporated, and a new one formed. The oxide layer can also influence the wetting angle if it forms at the three phase point, by pushing the sample towards the other edge. This can be observed in Figure 39c. The camera only gets picture from one side of the sample, therefore it is unclear what happens on the other sides.

The general trend in these results is that the wetting angle for the coated sample is a lot higher than the wetting angle for the non-coated samples. This can be seen in Figure 41. This shows that coating has a significant effect on the wetting angle.

5.3.3 General Observations

All 8 experiments on the non-coated samples melted perfectly, and all the 8 experiments on the coated had difficulty melting. This suggests that the coating causes the oxide

layer to form more easily. There are several possibilities of why this is happening. When heated above 600 ℃, the barium carbonate reacts with and creates barium silicate, as described in chapter 2.3, but there might also be some barium hydroxide left, which has not reacted, and is evaporating OH groups on to the melting silicon, which creates an oxide layer. The barium silicate that is in direct contact with the silicon might react with it, and the oxygen from the silicate can cause the formation of the oxide layer. Another possibility is that the cristobalite that is produced due to the coating is absorbed into the silicon, and the oxygen from the cristobalite is the oxygen source for the oxide layer.

When doing the same experiment with a non-coated sample at atmospheric pressure, an oxide layer is formed, just like with the coated samples in this thesis [32]. This is probably due to the silica that dissolves into the silicon, and creates an oxide layer when the oxygen reaches the surface. When the pressure in the furnace is lower, close to 20 mbar, the oxide layer evaporates faster than it is created. This does not happen to the coated samples in this thesis, meaning the amount of oxygen that goes through the system is greater than in the non-coated samples.

The wetting experiments were only done once for each combination of heat treatment and coating. This makes it hard to predict the uncertainty of the wetting angles. For the non-coated samples, the uncertainty in the wetting angle is probably not so large. The samples melted without any oxide layer formation, and was stable when melted. A standard deviation of less than one degree is proposed, and will not change the trend, and a clear effect between OH content and wetting angle can be seen based on this work. More extensive testing should be done to verify these results. For the coated samples the uncertainty is greater, due to an increase in factors that can vary. The formation of oxide greatly affects the wetting angle. Only one of the sides is observable, thus one cannot say anything about the amount of oxide layer on the other side. The coating might be uneven for some of the samples. Due to these factors, it is not possible to determine with certainty that the heat treatment has had any effect on the wetting angle on the coated samples.

5.4 Coating

The coating used in this work is thicker than the coating used industrially. The industrial coating can be seen in Figure 4. In this figure the coating layer is thin, and barium carbonate is easily seen as circular spots. The coating done in this work can be seen in Figure 43. In Figure 43a the barium carbonate can be seen as thick flakes on the surface, and in Figure 43b a closer look of the precipitated coating can be seen. The coating does have an effect on the formation of cristobalite nonetheless, as can be seen in Figure 44. The formation of cristobalite is considerably increased in the coated sample, as opposed to the non-coated sample. The wetting angle is also affected by the coating, as described previous. To get a better idea of the composition at the surface of the coated samples, other analyzing methods could have been used, for example electronic backscatter diffraction (EBSD) or X-ray diffraction (XRD), in order to make sure the coating was of industrial standard.

6 Conclusion

The results of this work indicates clearly that the OH content in the crucible samples is reduced when heat treated under vacuum conditions. These results are in agreement with literature. When heat treated at 1450 ℃ and above for 24 hours, the layer of cristobalite that forms is thick. This makes a crucible pretreated at these temperatures not suited for ingot pulling in the CZ process. For both crucible types tested in this work, the OH content was reduced to slightly above 30 ppm.

The crucible samples are obtained from an industrial manufacturer. The results of this work suggest that the wetting angle is affected by the OH content in the non-coated crucibles. It is not possible to say if the OH content affects the wetting angle for coated samples, due to a large amount varying factors that might play a bigger part when it comes to the wetting angle. However, coated samples do have a generally larger wetting angle than the non-coated crucible.

In conclusion, heat treating a crucible at the temperatures and holding times used in this work will not alone make a liquinert crucible. The removal of OH groups will however reduce the wettability between the silica crucible and the silicon melt, and might be a step in the direction of creating a liquinert crucible.

7 Further work

When considering further work, finding out where in the temperature range from 1400 ℃ to 1450 ℃ the cristobalite formation starts to be significant. Increasing the holding time at the temperatures used in this work would also be interesting when considering OH removal. It should also be investigated how great the effect is when the holding time is increased to 100 hours at 1400 ℃. More experiments should be conducted, to test the reproducibility of the work done in this thesis. The removal of OH is probably not the only step in creating a liquinert crucible. Other kind surface treatments should be investigated.

References

[1] Fraunhofer ISE Dr. Simon Philipps. Photovoltaics report, July 12 2017.

[2] John Atle Bones. Conversation with SINTEF Solar cell researcher J.A. Bones, spring 2018.

[3] The quartz page: Introduction. `http://www.quartzpage.de/intro.html`. (Accessed on 05/19/2018).

[4] Ove Paulsen SINTEF Materialer og kjemi. "memo - fused silica cz-crucibles", 2014.

[5] The quartz page: The silica group. `http://www.quartzpage.de/gen_mod.html`. (Accessed on 02/19/2018).

[6] Czochralski process - wikipedia. `https://en.wikipedia.org/wiki/Czochralski_process`. (Accessed on 02/11/2018).

[7] Fabrication of the single crystal - waferfabrication - semiconductor technology from a to z - halbleiter.org. `https://www.halbleiter.org/en/waferfabrication/singlecrystal/#Czochralski_process`. (Accessed on 03/12/2018).

[8] What is the czochralski process? `http://www.top-alternative-energy-sources.com/Czochralski-process.html`. (Accessed on 06/27/2018).

[9] Xinming Huang, Shinji Koh, Kehui Wu, Mingwei Chen, Takeshi Hoshikawa, Keigo Hoshikawa, and Satoshi Uda. Reaction at the interface between si melt and a ba-doped silica crucible. *Journal of crystal growth*, 277(1-4):154–161, 2005.

[10] Xinming Huang, Takeshi Hoshikawa, and Satoshi Uda. Analysis of the reaction at the interface between si melt and ba-doped silica glass. *Journal of Crystal Growth*, 306(2):422–427, 2007.

[11] The application of barium hydroxide in quartz crucible coating. `http://www.bmschem.com/servicesaxx_en/id/180.html`. (Accessed on 06/22/2018).

[12] Helene Elisabeth J Hendrickx. Cristobalite formation on quartz crucibles inner surface for cz solar cell ingot production. Master's thesis, NTNU, 2017.

[13] David R Brown, Charles E Frost Jr, and Kenneth A White. Method of manufacturing quartz glass crucibles with low bubble content, December 30 1986. US Patent 4,632,686.

[14] Tetsuo Fukuda, Yukichi Horioka, Nobutaka Suzuki, Masaaki Moriya, Katsuto Tanahashi, Shalamujiang Simayi, Katsuhiko Shirasawa, and Hidetaka Takato. Lifetime improvement of photovoltaic silicon crystals grown by czochralski technique using "liquinert" quartz crucibles. *Journal of Crystal Growth*, 438:76–80, 2016.

[15] William. Callister and David. Rethwisch. *Materials Science and Engineering: An Introduction*. Wiley, 2010.

[16] Types of chromatography. https://www.slideshare.net/fizanchee/types-of-chromatography. (Accessed on 03/18/2018).

[17] Anthony Moulson and James Roberts. Water in silica glass. *Transactions of the Faraday Society*, 57:1208–1216, 1961.

[18] Hajimu Wakabayashi and Minoru Tomozawa. Diffusion of water into silica glass at low temperature. *Journal of the American Ceramic Society*, 72(10):1850–1855, 1989.

[19] Yukihiro Morimoto, Tastushi Igarashi, Hiroshi Sugahara, and Shoichi Nasu. Analysis of gas release from vitreous silica. *Journal of non-crystalline solids*, 139:35–46, 1992.

[20] Zhou Yongheng and Gu Zhenan. The study of removing hydroxyl from silica glass. *Journal of non-crystalline solids*, 352(38):4030–4033, 2006.

[21] Astrid Marie Muggerud. Conversation with The Quartz Corp representative, A.M.F Muggerud, spring 2018.

[22] Preben C. Mørk. *Surface and colloid chemistry. Basic principles and theories*, volume 8. NTNU, 2004.

[23] Sarina Bao, Kai Tang, Anne Kvithyld, Merete Tangstad, and Thorvald Abel Engh. Wettability of aluminum on alumina. *Metallurgical and materials transactions B*, 42(6):1358–1366, 2011.

[24] Daniel Weiß, Tim Gebensleben, Lisa Diestel, Lukas Alphei, Verena Becker, and Jörg August Becker. The influence of crystallographic orientation on the wetting of silicon on quartz single crystals. *Journal of materials science*, 46(10):3436–3444, 2011.

[25] Lucas Alphei, Robin Grotjahn, Mark Douvidzon, Tim Gebensleben, Tim Alznauer, Victor Becker, and Jörg August Becker. Relating wetting and reduction processes in the si-liquid/sio2-solid interface. *Journal of Crystal Growth*, 419:165–171, 2015.

[26] How an FTIR Spectrometer Operates - Chemistry LibreTexts. `https://chem.libretexts.org/Core/Physical_and_Theoretical_Chemistry/Spectroscopy/Vibrational_Spectroscopy/Infrared_Spectroscopy/How_an_FTIR_Spectrometer_Operates`. (Accessed on 03/03/2018).

[27] Introduction - aims and learning outcomes — myscope. `http://www.ammrf.org.au/myscope/sem/introduction/`. (Accessed on 06/03/2018).

[28] How an sem works. `https://www.nanoscience.com/technology/sem-technology/how-sem-works/`. (Accessed on 06/17/2018).

[29] Scanning electron microscope (sem) & how it works — scanning electron microscopy@unimap. `http://emicroscope.blogspot.com/2011/03/scanning-electron-microscope-sem-how-it.html`. (Accessed on 06/17/2018).

[30] Ivan Fanderlik. *Silica Glass and Its Application*. Elsevier, 2013.

[31] Bert Sloots. Measuring the low OH content in quartz glass. *Vibrational Spectroscopy*, 48(1):158–161, 2008.

[32] M Strømmen. How water content effects the wetting of silicon on quartz, December 2017.

[33] Device and method for coating quartz crucible barium hydroxide. `https://patents.google.com/patent/CN102336527A/en`. (Accessed on 05/13/2018).

[34] Standard deviation formulas. `https://www.mathsisfun.com/data/standard-deviation-formulas.html`. (Accessed on 06/28/2018).

A Appendix

A.1 Chemical concentration of impurities in samples

Table 6: Concentration of impurities in the natural and synthetic silica samples, in ppm %w[0].

	Natural	Synthetic		Natural	Synthetic
Al	13	<1	Mg	0.02	0.03
B	<0.1	NA	Mn	0.03	0.03
Ca	0.6	<0.1	Na	0.7	0.3
Cr	0.06	0.007	Ni	<0.01	0.02
Cu	0.02	0.02	Pt	NA	NA
Fe	0.17	0.17	Ti	1.3	<0.1
K	0.3	0.2	Zn	<0.01	0.01
Li	0.4	0.2	OH	NA	NA

A.2 Matlab script

```
data = load('DataFromFTIR.dpt');
y = data(1:length(data),2);
x=data(1:length(data),1);
[ycorrect, baseline] = bf(y,5,'confirm');
d = 1.25;
Tmin = min(1-abs(ycorrect));
beta=(1/d)*log(1/Tmin);
factor = (17*10000)/(77.5*2.21);
OHppm=factor*beta;
```

A.3 FTIR Spectra for all samples

[0]NA=Not Available

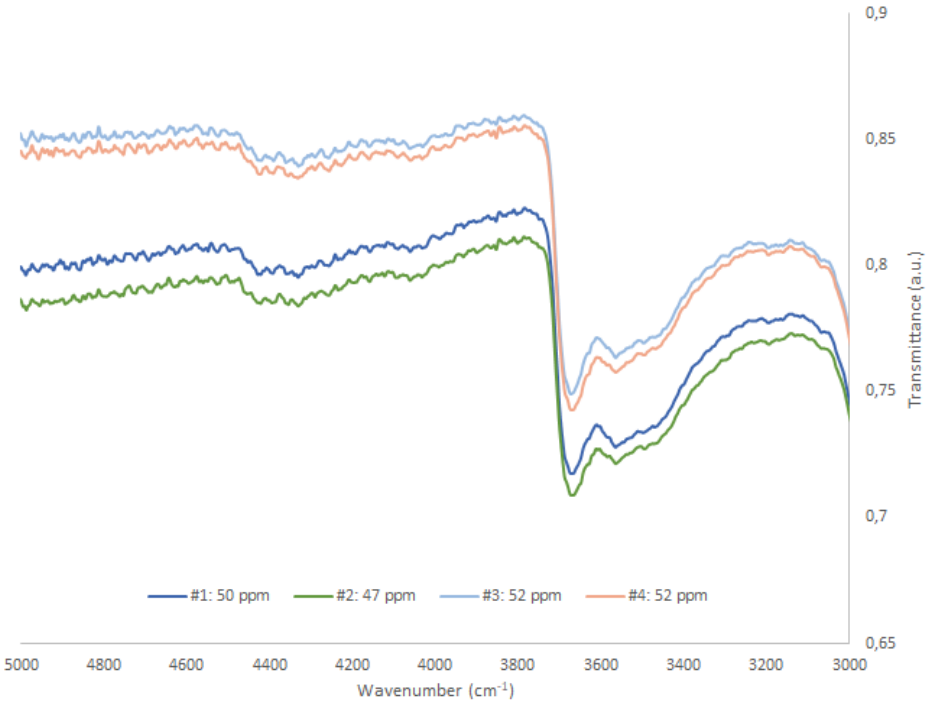

Figure 45: FTIR spectra with given oxygen calculated for untreated natural samples

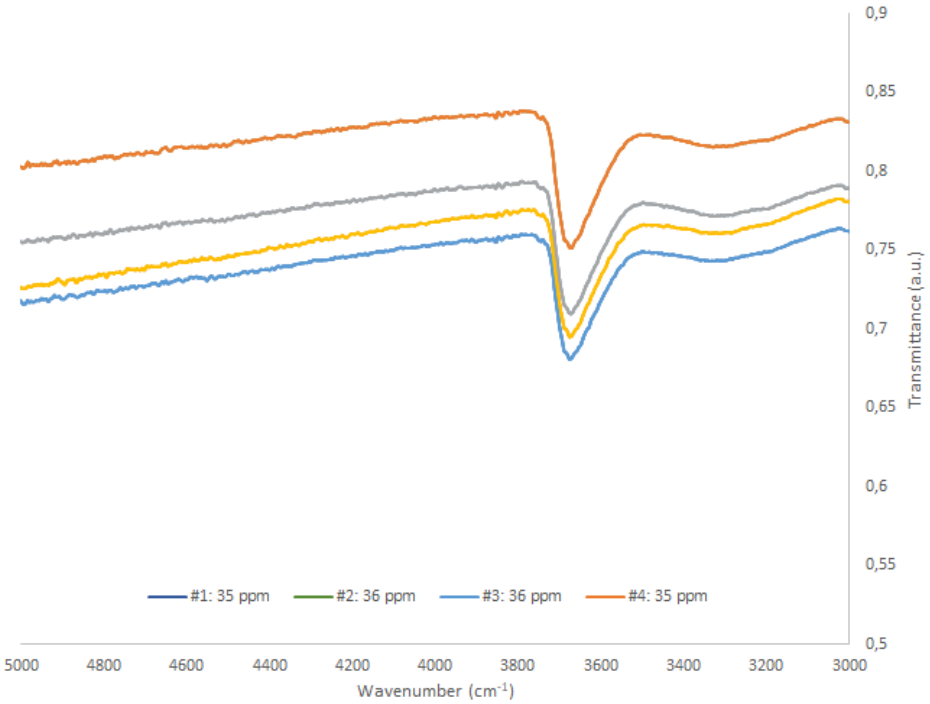

Figure 46: FTIR spectra with given oxygen calculated for natural samples heat treated at 1350 ℃ for 24 hours

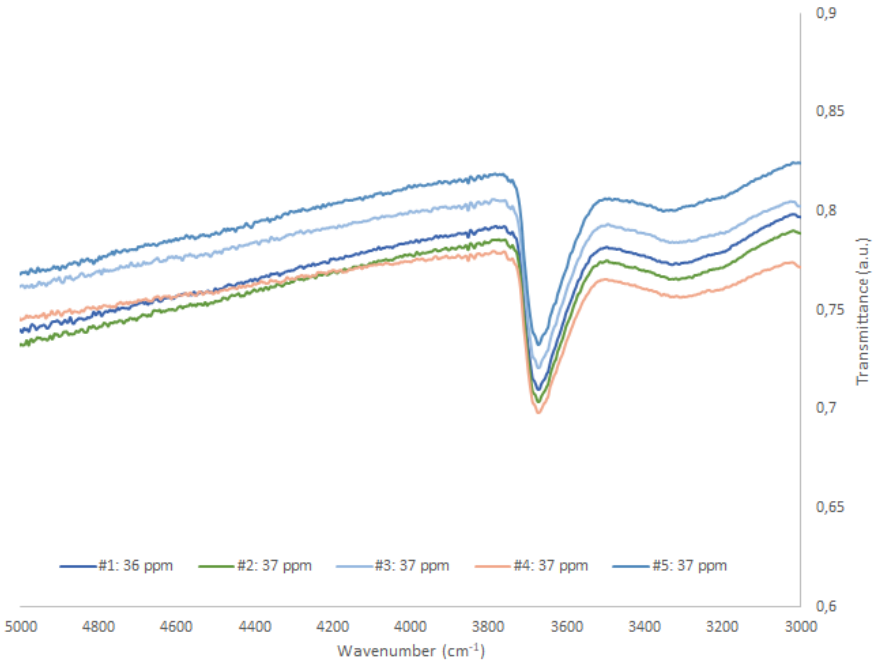

Figure 47: FTIR spectra with given oxygen calculated for natural samples heat treated at 1400 ℃ for 24 hours

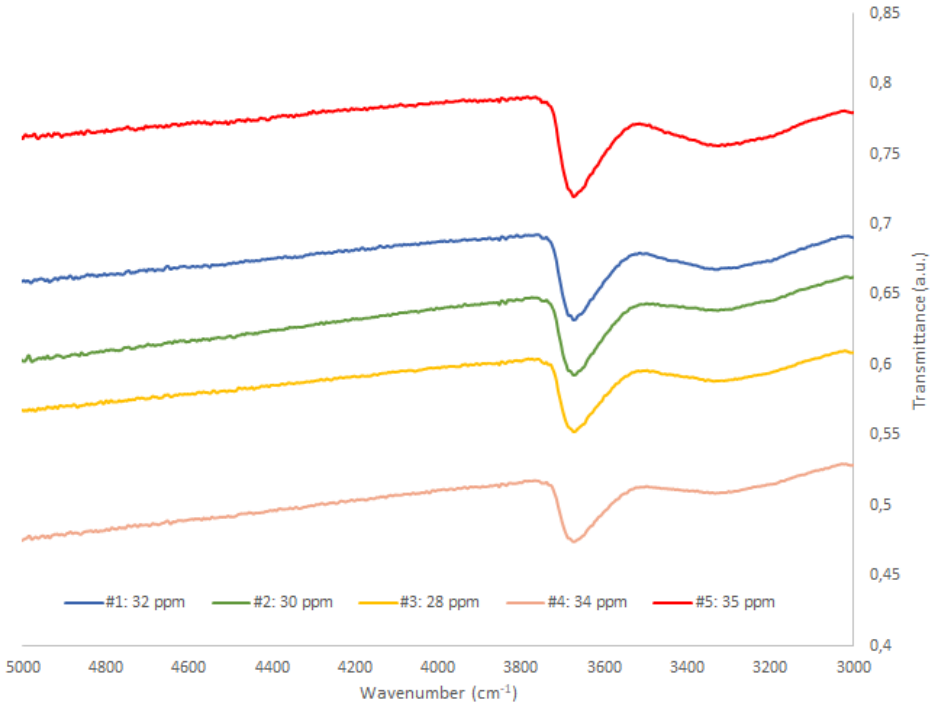

Figure 48: FTIR spectra with given oxygen calculated for natural samples heat treated at 1450 ℃ for 24 hours

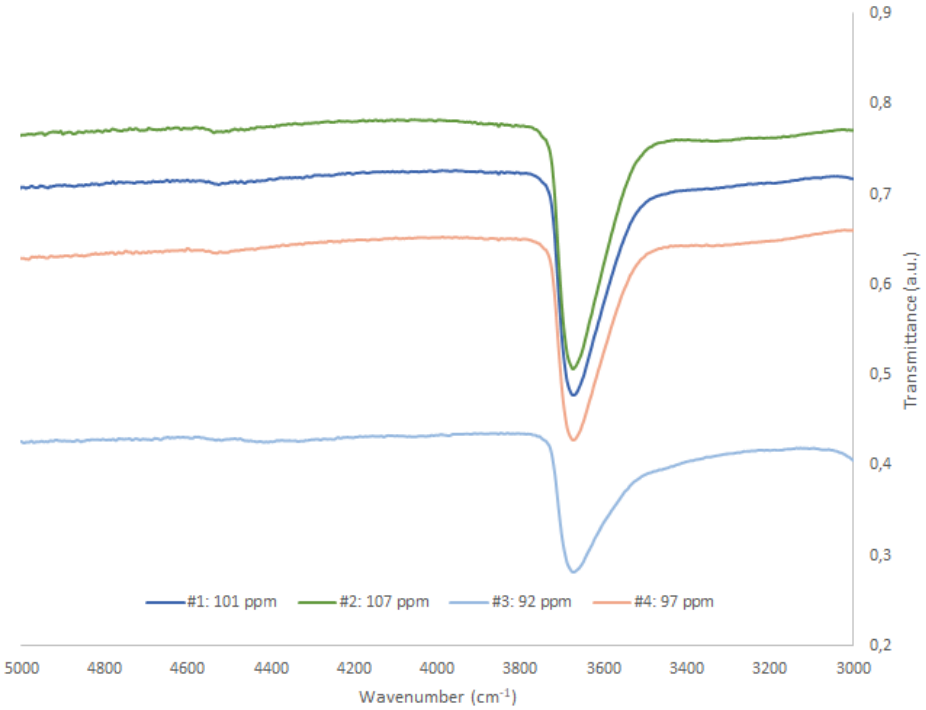

Figure 49: FTIR spectra with given oxygen calculated for untreated synthetic samples

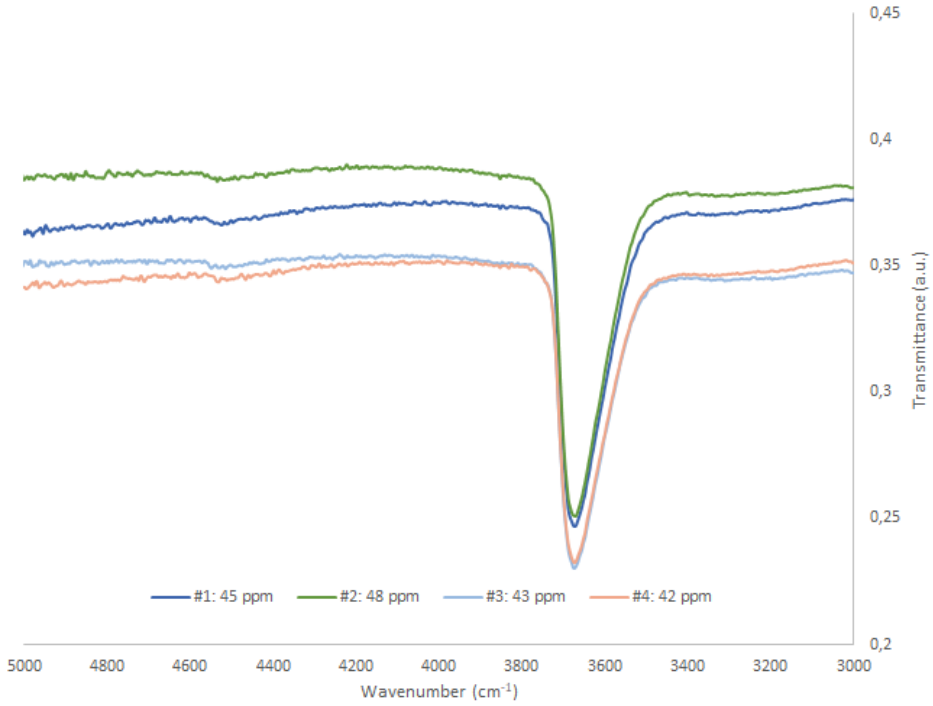

Figure 50: FTIR spectra with given oxygen calculated for synthetic samples heat treated at 1350 ℃ for 24 hours

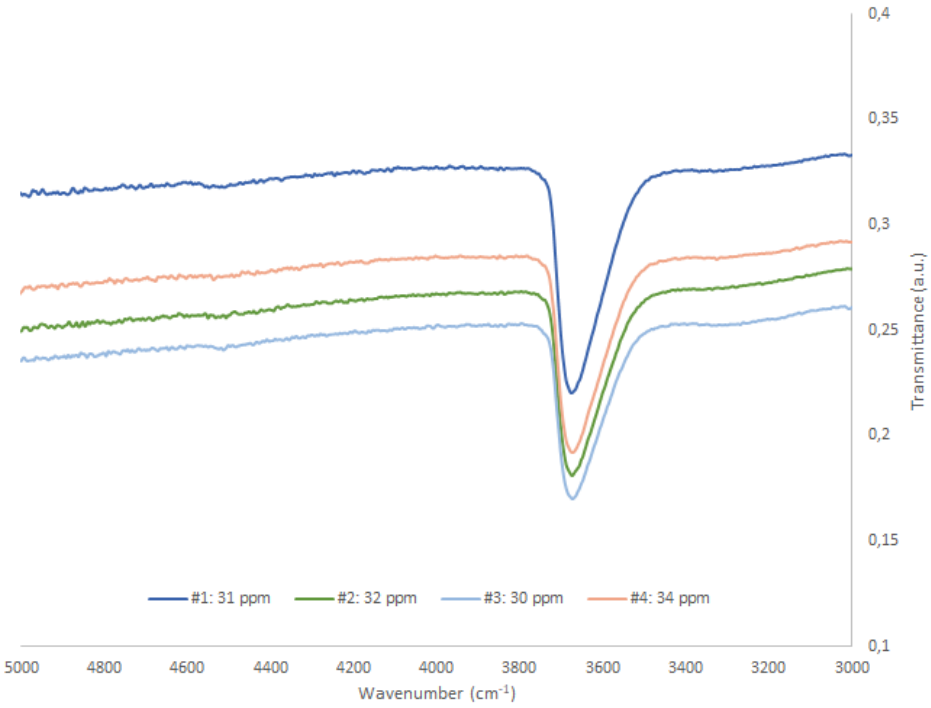

Figure 51: FTIR spectra with given oxygen calculated for synthetic samples heat treated at 1400 ℃ for 24 hours